Voltage Induced Variation of Solid Acid Catalyst Acidity

A Major Qualifying Report
Submitted to the Faculty
of the
WORCESTER POLYTECHNIC INSTITUTE
in Partial Fulfillment of the Requirements for the
Degree of Bachelor of Science
in Chemical Engineering

Rexford Hoadley
Jonathan Vardner
Project Advisor: Professor Michael Timko
Co Advisor: Professor Christopher Lambert

Abstract

The decomposition of biomass is an attractive energy alternative for the 21st century. In biomass conversion, acid groups catalyze the degradation of cellulose to form glucose. Liquid phase acid catalysts are commonly used for biomass decomposition; however solid acid may be a more cost-effective approach since they obviate the need for dilute acid pretreatment. Currently, the required acidity of solid acid catalysts to hydrolyze cellulose is unknown. Here, we attempt to develop an electrochemical technique that effectively varies the acidity of solid acid catalysts. We applied voltage offsets to acidic self-assembled monolayers (SAMs) at varying pH levels and characterized the fraction of protonated acid groups with potentiostatic electrochemical impedance spectroscopy (EIS). The results indicated that self-assembled monolayers (SAMs) degraded under the experimental conditions, and therefore, the factors that contributed to the stability of SAMs were investigated. Ultimately, we aim to determine the required acidic conditions that result in biomass deconstruction.

Table of Contents

1.0 Introduction

Particles are comprised of surface atoms and bulk atoms. Chemical and physical processes occur at the surface atoms, rather than the bulk atoms, in fields such as catalysis, optics, and electronics. Therefore, it is often desirable to maximize the fraction of surface atoms in materials. In recent decades, advancements in nanoscience have led to the synthesis of nano-sized particles, which have greater fractions of surface atoms than their bulk-sized counterparts. Resulting from their increased surface areas, nanoparticles often actuate surface processes more efficiently than bulk-sized particles (Love et al. 2005). Furthermore, nanoparticles may exhibit unique properties that result from their high fraction of surface atoms. In atomic clusters, surface atoms can have different coordination numbers than bulk atoms, and consequently, surface atoms can have different free energies, electronic states, and reactivities. In some instances, the coordination numbers of surface atoms lead to enhancement in surface processes (Hvolbæk et al. 2007).

Additionally, the surfaces of particles can be engineered to exhibit a wide range of properties; self-assembly, in particular, has attracted great interest for surface modification. A self-assembled monolayer (SAM) is a nanostructure that spontaneously adsorbs to a substrate and organizes into a highly organized array. SAMs have applications such as metal protection from degradation, blockage of electron transport, and resistance of protein in biological systems. SAMs consist of three components: a head group, a tail, and a functional group. The head group anchors the SAM to the substrate due to its strong affinity with the substrate. The tail, commonly an alkyl chain, separates the head group from the functional group. Lastly, the functional group regulates the interfacial properties of the SAM and can be tailored to promote desired properties. Thiol-based SAMs adsorbed to gold substrates have become a standard for many studies since they produce stable, compact, and flexible coatings on surfaces (González-Granados et al. 2013). Carboxylic acid thiols, for instance, have been used for protein adsorption and biological sensing purposes (Love et al. 2005).

In recent decades, the study of modified surfaces on electrodes has gained much attention. Electrochemists have studied modified surfaces on electrodes to elucidate fundamental processes and to develop practical applications. For instance, electrochemists have studied the effect of electrode potential on surface acid-base properties. Smith and White (1993) first reported the reversible, potential-driven protonation-deprotonation effect of acidic SAMs adsorbed to a gold

substrate. These authors determined that the deprotonation of an acidic head group follows the expression below at thermodynamic equilibrium.

$$\ln\left(\frac{\theta}{1-\theta}\right) = pH - pk_a + \frac{F\phi_{SAM}}{RT}$$

In this expression, θ represents the fraction of deprotonated head groups, pKa is the surface pKa of the bound thiol, F is the faraday constant, ϕ_{SAM} is the potential at the surface of the SAM, R is the gas constant, and T is the temperature. This expression is similar to the Henderson-Hasselbalch equation; however unlike the Henderson-Hasselbalch equation, this expression has a term to account for the presence of an electric field. Fawcett et al. (1994) extended this model to include a more accurate Stern layer, and furthermore, Andreu and Fawcett (1994) extended the model to account for the discreetness of charge effects at the molecular films.

Experimentally, Bryant and Crooks (1993) first reported the potential driven deprotonation of carboxylic SAMs using 4-mercaptopyridine and 4-aminothiophenol adsorbed to a gold wire. Shortly after, White et al. (1998) reported the potential driven deprotonation of carboxylic SAMs using 11-mercaptodecanoic acid backfilled with 1-decanethiol on a silver (111) substrate. Sugihara et al. (2000) substantiated the findings by reporting the shift in pKa of 15-mercaptohexadecanoic acid with applied voltage. Lastly, Cao (2005) investigated the protonation of amino groups using Fourier transform surface-enhanced raman spectroscopy.

Electrochemical impedance spectroscopy (EIS) has been utilized to characterize the protonation-deprotonation effect of SAMs in the literature. Kakiuchi et al. (2000) used EIS to investigate the effect of carbon chain length on capacitance over a pH range of 2-12 pH units. These authors determined that long carbon chain lengths yield constant capacitance with pH, whereas short chain lengths yield varying capacitance with pH. Furthermore, Burgess et al. (2006) used EIS to measure the voltammetric peak height for voltage-driven protonation and deprotonation.

In this experiment, our primary aim is to determine the protonation-deprotonation effect for sulfonic acid SAMs adsorbed to gold substrates. As shown below in Fig. 1, SAMs interact with the bulk solution through an interfacial double layer, which is formed as ions in solution interact with the SAM. The protons bonded to the SAM dissociate when their chemical potential are

equivalent to the chemical potential of protons in the interfacial double layer. The chemical potential of protons depends on the bulk solution pH as well as the applied voltage to the substrate; therefore the fraction of protonated acid groups also depend on the bulk solution pH and application of voltage. The charged SAM-adsorbed electrode is separated by the charged ions in the interfacial double layer by a small insulating space. The separation of charges yields a capacitor. The capacitance depends on the ions in the double layer as well as the charge of the SAM-adsorbed electrode. Consequently, the capacitance can be measured to determine the fraction of protonated acids of the SAM.

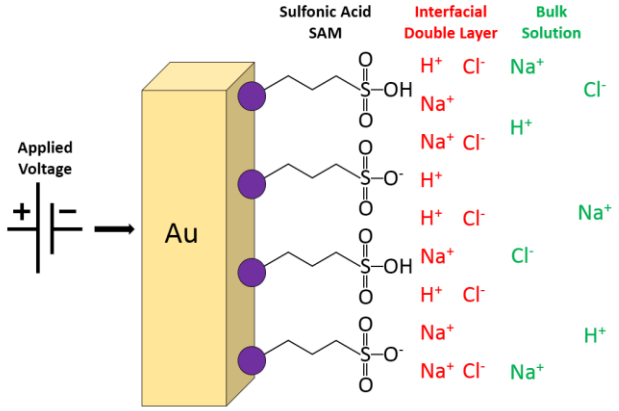

Fig 1. Depiction of sulfonic acid thiols adsorbed to a gold substrate. The fraction of protonated acidic groups depends on bulk solution pH and applied voltage.

The potential induced protonation-deprotonation effect may be useful in the study of solid acid catalysts for cellulose hydrolysis. Solid acid catalysts are gaining attention for biomass decomposition because they obviate the need for dilute-acid pretreatment, and therefore, are an economically attractive alternative to liquid-phase catalysts. Little research has been conducted to optimize the use of solid acid catalysts, however. No experiment, for instance, has been conducted to determine the required acidity for solid acid catalysts to hydrolyze cellulose. Potential-controlled variation of acidity on SAMs is a viable option to systematically change the pKa of SAMs in small increments. We aim to vary the pKa of SAMs containing sulfonic acid head groups because these SAMs are known to effectively catalyze cellulose hydrolysis. Here, we attempt to stabilize sulfonic acid thiols on gold surfaces so that sulfonic acid thiols, ultimately, can be used more effectively in hydrolysis experiments.

2.0 Methodology

Initially, potentiostatic electrochemical impedance spectroscopy (EIS) was used to investigate the pKa of acidic SAMs adsorbed to gold substrates at varying voltage offsets. We conducted EIS using a Gamry Reference 600. The SAMs, however, deteriorated during the EIS trials, and therefore, the scope of the project diverged to the investigation of factors that contribute to overall SAM stability. Here, we present the methodology for the synthesis of SAMs pH titration tests at varying voltage offsets, and SAM stability tests.

2.1 Synthesis of SAMs

SAMs were prepared based on the thesis of Milkani (2010). The preparation of SAMS consisted of three steps: (1) the cleaning of a substrate, (2) the preparation of a SAM solution, and (3) the adsorption of molecules to the substrate. The majority of experiments were conducted with thiol-based-SAMs adsorbed to gold substrates; however silanes adsorbed to indium tin oxide (ITO) substrates were also briefly examined.

Gold slides purchased from EMF were cut into seven rectangular 2.5cm x 1.0cm pieces to increase the number of experiments per gold slide. First, gold pieces were cleaned in a piranha solution (70% sulfuric acid, 30% hydrogen peroxide) for 10 minutes. The time span of 10 minutes was chosen to permit the oxidation of organic matter and to prevent the destruction of the thin gold layer. The gold pieces were then rinsed with deionized water and ethanol, and subsequently, the pieces were dried with nitrogen gas. Lastly, the gold pieces were cleaned in oxygen plasma for 45 seconds. The ITO slides (Delta Technologies, Limited) were cut into seven pieces, sonicated, and cleaned with oxygen plasma.

A SAM solution was prepared with a selected solute and solvent. The solute was selected for its functional properties and the solvent was selected for its ability to dissolve the particular solute. The solutes included 1-octanethiol, 11-mercaptoundecanoic acid, 4-mercaptobutyric acid, 3-mercatopropylsilane, and sodium 3-mercapto-1-propanesulfonate. These solutes were selected based on their acidic properties, carbon chain length, and strength of adsorption to a substrate. The solutes were typically dissolved in ethanol at a concentration of 1 mM. The carboxylic acid SAMs,

however, were also prepared in a solution of ethanol and 2% (v/v) trifluoroacetic acid (TFA) for some trials. TFA was included to prevent carboxyl head groups from hydrogen bonding during SAM formation. Hydrogen bonds can form dimers of acid, affecting the SAM quality. Furthermore, 3-sulfonic acid was prepared in methanol at a concentration of 0.4g/L for some trials because this solution was uses successfully in the literature (Ashwell et al. 2006).

The cleaned substrates, followed by approximately 20 ml of the SAM solution, were placed in a cylindrical glass container. A cover was placed on the container, and the unit was sealed with parafilm to prevent atmospheric water vapor from contaminating the solution. Substrates immersed in solution were typically stirred for a duration of 12 hours. Stirring times ranging from five hours to 16 hours were also examined to identify the ideal stirring time. The solution was placed under a black cover throughout the stirring duration to prevent light exposure. After the appropriate amount of time had passed, the gold substrates were rinsed with ethanol, and the ITO substrates were rinsed with chloroform followed by ethanol to remove residual chemicals. Substrates in a solution containing TFA were also rinsed with 10% (v/v) ammonium hydroxide in ethanol to remove TFA from the surface. Lastly, the substrates were dried with a stream of nitrogen gas and then sealed in a plastic container with parafilm. For some experiments, the substrates were backfilled with 1-octanethiol to increase the structural stability of the SAM. It may be beneficial in future experiments to prepare mixed monolayers with an acidic SAM and an alkanethiol to further increase SAM stability, as conducted in the literature (White et al. 1998).

2.2 pH Titration Tests at Varying Voltage Offsets

SAMs were typically characterized by contact angle measurements with a Rame-hart instrument to verify the presence of the SAM on the substrate, according to the literature (Smith et al. 2004). Contact Angle measurements of about 30, 15, and 30 in acid, base, and water, respectively were characteristic for a SAM-adsorbed substrate. Contact Angle measurements of 60-70 in acid, base, and water were characteristic for a substrate without a well-formed SAM. It should be noted, however, that there was some variation in the contact and measurements between trials.

A solution of 0.1M NaCl (Sigma Aldrich) in water was prepared and placed into a four-port cell, as pictured in Fig. 2. The concentration of salt affects the capacitance measurements;

therefore the salt concentration was consistent throughout all trials (Schweiss et al. 2003). The pH of the solution was measured using a pH meter (Denver Instruments). The platinum counter electrode, camomile reference electrode, and nitrogen needle were inserted into their respective ports of the cell. Parafilm was used to seal the remaining port for the working electrode as well as any space exposed to the atmosphere. Nitrogen bubbled though the NaCl solution for approximately one hour to remove atmospheric oxygen from solution. The working electrode was then inserted through the remaining port, facing the counter electrode, and was subsequently sealed with parafilm. One cm^2 of the substrate was immersed in the NaCl solution.

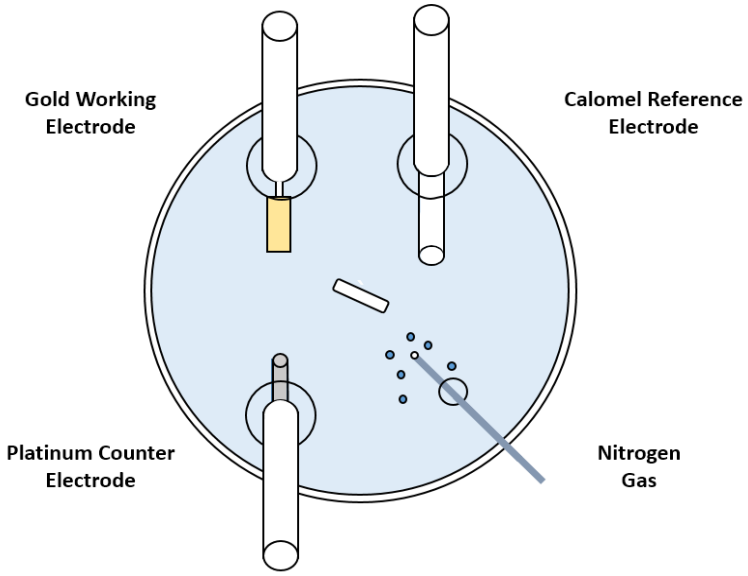

Fig. 2. Orientation of electrodes and nitrogen needle for EIS experiments.

Typically, during EIS measurements, a 5 mV perturbation voltage was applied to the gold substrate over a frequency range of 1 Hz to 100,000 Hz. The perturbation voltage and frequency range was altered for some trials to better understand the effects of these parameters. The pH was varied by removing the counter electrode, removing known volumes of the NaCl solution, and adding equivalent volumes of either 0.1M HCl or 0.1M NaCl. Equivalent volumes were removed as added to keep the volume of solution, and thus the area of submerged substrate, constant. The new pH of the solution was measured, and subsequently, the counter electrode was reinserted into the port and was resealed with parafilm. Nitrogen was allowed to bubble throughout the solution for approximately 15 minutes between pH adjustments since the solution was exposed to the

atmosphere for some time. The bubbling rate was kept low between pH adjustments because high flows of nitrogen would result in liquid contacting the clip holding the working electrode, which would result in immeasurable EIS readings. For some trials, a duration of 30 minutes of nitrogen degassing was allowed between pH measurements to make complete oxygen removal more probable. We typically applied a -0.1V, 0V, and a 0.1V offset voltage at each pH measurement. The pH adjustment and application of offset voltage were conducted in random orders. Therefore trends in the results did not depend on the order of pH adjustments or the application of voltage.

The collected data in the Bode and Nyqust plots were fit with equivalent circuit models to estimate the double-layer capacitance using Gamry's Echem Analyst. The capacitance measurement was practical because it collapsed the numerous data throughout the measured frequency range to a single point of data. The thin films of this experiment did not behave as perfect capacitors due to imperfections in capacitance distribution, and therefore, the circuit model was chosen to account for the nonideality. The constant phase element (CPE) circuit model was found to most accurately fit the obtained data at various pH values and voltage offsets. Capacitance was extracted from the CPE circuit model with the following relationship:

$$C = \sqrt[\alpha]{\frac{Y_o}{R_{SAM} + R_{SOLN}}}$$

In this expression, C represents the capacitance, Y_o represents the CPE, R_{SAM} represents the SAM resistance, R_{SOLN} represents the solution resistance, and α represents a fractional term dictating the nonideality of the capacitor. Gamry's Echem Analyst determined Y_o, R_{SAM}, R_{SOLN}, and α by applying a model of best fit to the raw data.

2.3 SAM Stability Tests

The degradation of SAMs was measured using cyclic voltammetry (CV). In CV, the potential of the working electrode is cycled through specified values, and the current transferred to the counter electrode is measured. Well-ordered SAMs resist the flow of current, resulting in low current measurements in CV. Degraded SAM's, however, do not resist the flow of current well, resulting in high current measurements in CV.

To perform CV, a solution containing 1mM potassium ferricyanide (Sigma-Aldrich) and 0.1M KCl (Sigma-Aldrich) in water was prepared. The solution was typically placed in a 150 mL beaker due to the lack of a second four-port cell. For some trials, however, the solution was prepared in the cell to ensure that atmospheric oxygen did not greatly affect the results. Like EIS, the electrodes were positioned in the solution and the solution was degassed with nitrogen. The reduction-oxidation potential of ferrocyaide was determined to be 0.216 V, and therefore, the voltage was cycled between a minimum value of 0.15 V and a maximum value of 0.35 V.

The degradation was quantified by the difference in height between the reduction peak and the oxidation peak. A pure gold slide was considered to represent 100% degradation of SAM. Therefore, the difference between peak heights of the SAM was divided by the difference in peak heights of pure gold to determine fractions of SAM degradation.

The SAM stability tests were used to confirm the degradation of SAMs in EIS experiments. The SAM stability tests were then used to identify the conditions that result in SAM degradation. It may be beneficial in future work to solely use a ferricyanide solution for pH titration and stability testing in order to reduce degassing times. This approach is atypical but has been conducted successfully in the literature (Raj and Behera 2005).

3.0 Results

Here, we present the results for the pH titration sets at varying voltage offsets as well as the SAM stability tests. Throughout the experiment we used various acidic SAMs and operating conditions. The flow chart below summarizes our motivations and findings for experiments.

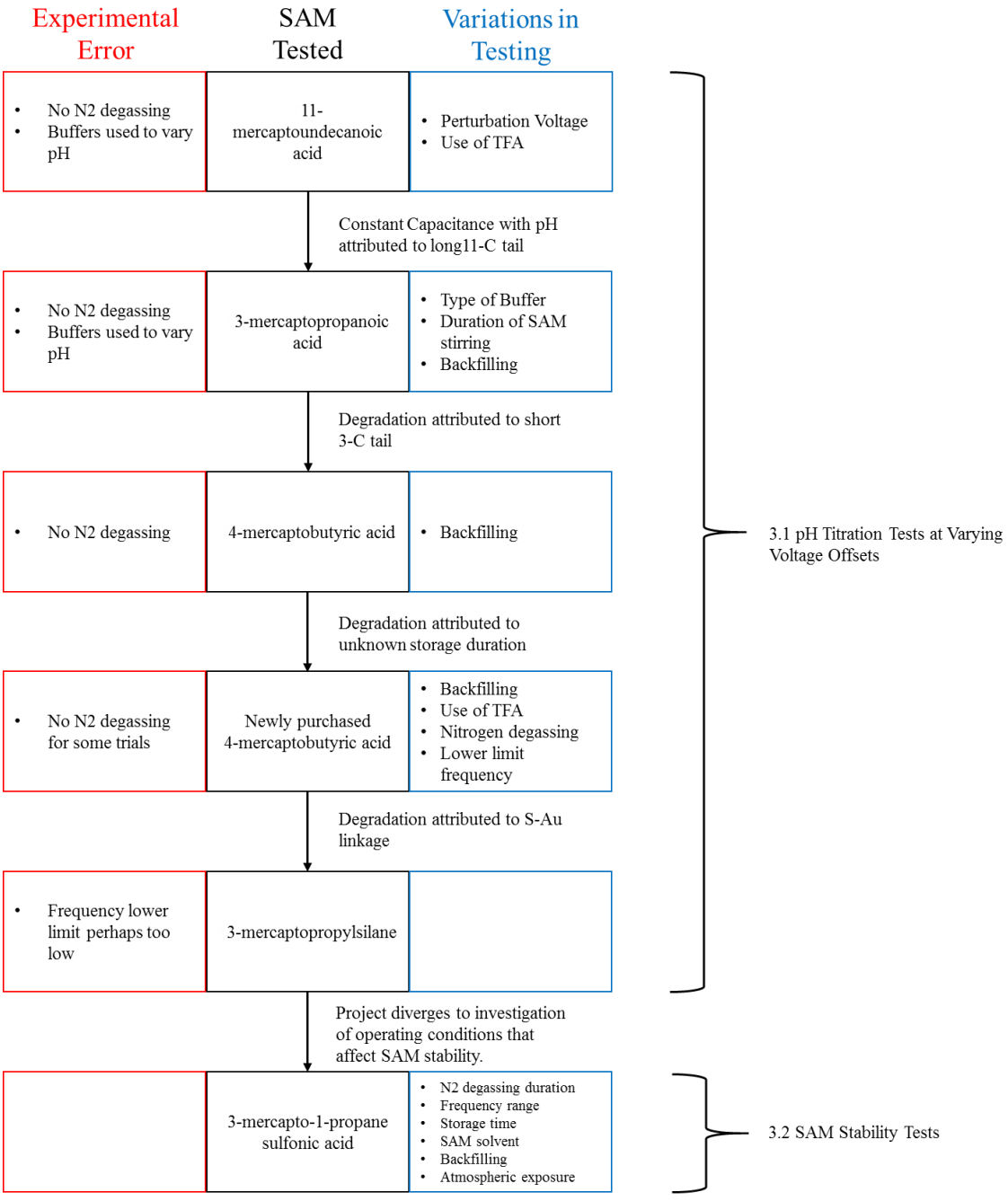

Fig. 3. Flowchart schematic of results

3.1 pH Titration Tests at Varying Voltage Offsets

Initially, pH titration tests with varying voltage offsets were performed using the SAM, 11-mercaptoundecanoic acid, adsorbed to a gold substrate. Contact angle measurements of about 30, 15, and 30 in acid, base, and water, respectively indicated the adsorption of the SAM. EIS measurements were run to investigate the shift in phase angle with frequency at varying pH values and varying voltage offsets. These data were modeled with circuit models to determine capacitance, and therefore, these data of phase angle vs frequency demonstrate the variation of capacitance. The results for one trial, using 11-mercaptoundecanoic acid, are depicted in Fig. 4 below. The results for other trials are presented in the appendix.

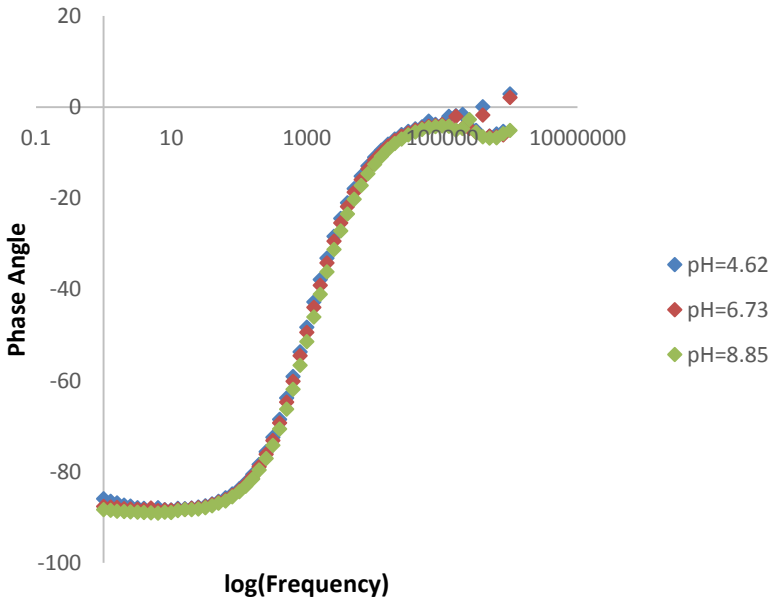

Fig. 4. 11-mercaptoundecanoic acid tested at 0.1V offset for 3 pH values

These data indicate that variations in pH and voltage offset have no measurable effect on the SAM-solution interfacial layer. It is important to note that these trials were conducted without nitrogen degassing and with a buffer to vary pH. We deemed that the 11-carbon tail of the SAM prevented variation in capacitance measurements. Consequently, we started to use the SAM, 3-mercaptoprotoanoic acid, since this SAM has a shorter tail length. The results for one trial using 3-mercaptoprotoanoic acid are depicted in Fig. 5 below.

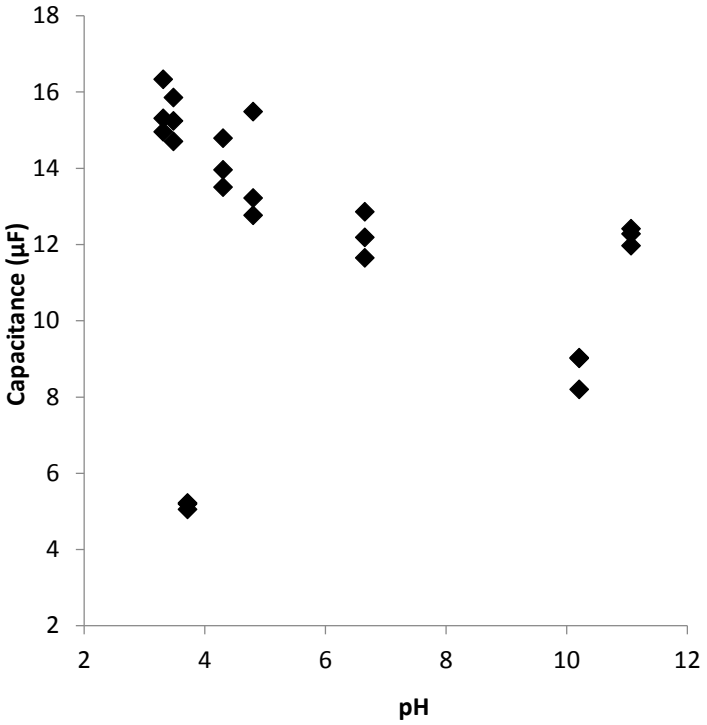

Fig. 5. 3-mercaptopropanic acid made in TFA backfilled with 1-octanethiol tested in HCl, NaOH, NaCl

The EIS results, again, were inconsistent with the literature (Kakiuchi et al. 2000). Furthermore, contact angle measurements before and after the pH titration indicated that the SAM had degraded during the experiment. It should be noted that these trials, as well, were conducted without nitrogen degassing. Operating conditions such as the use of TFA in the SAM solution, the use of buffers, and backfilling electrodes with 1-octanethiol were varied; however each set of operating conditions led to SAM degradation. We attributed the degradation of the SAM to the short 3-carbon tail. The work of Dai and Ju (2001) indicates that 4-carbon tails yield much more stable SAMs than 3-carbon tails. Therefore, we then conducted experiments with 4-mercaptobutyric acid as shown below in Fig. 6.

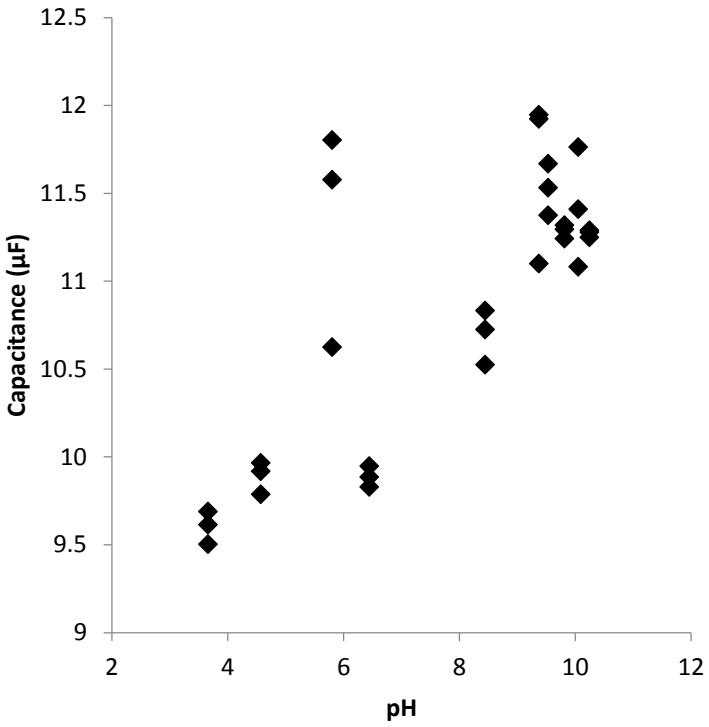

Fig. 6. Old 4-mercaptobutyric acid SAM made in ethanol with TFA tested at 0V in HCl, NaOH, NaCl

The contact angle measurements indicated that these SAMs degraded as well. We attributed the degradation of SAMs to their unknown storing durations. Since we did not purchase 3-mercaptoprotoanoic acid or 4-mercaptobutyric acid, it was possible that the chemicals had lost their potency from storage duration or mishandling. It was also possible that we had simply received poor batches of the chemicals. Therefore, we purchased 4-mercaptobutyric acid (Sigma Aldrich) to preclude these potential issues. The results for one trial using newly purchased 4-mercaptobutyric acid are depicted in Fig. 7 below. The results for other trials are presented in the appendix.

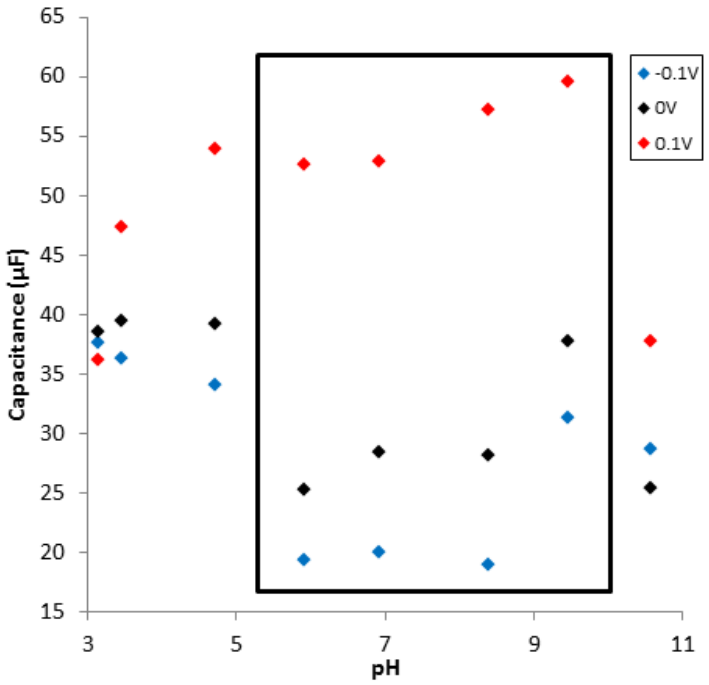

Fig. 7. pH titration curve for 4-mercaptobutyric acid SAM adsorbed to a gold substrate at varying voltage offsets. The data points outlined by the rectangular region represent the first four pH titrations.

The results for pH titration tests were not consistent with the literature (Kakiuchi et al. 2000). The first few EIS trials, however, often had the same general trend as the literature. For instance, in Fig. 7 above, the capacitance increased with pH at constant voltage for the first 16 EIS trials (outlined by the rectangular region) using a 4-mercaptobutyric acid SAM. The results of Fig. 3 indicated that the SAM was prone to degrade due to some condition(s) during experimentation. CV's before and after the titration were used to confirm SAM degradation as shown below in Fig. 8.

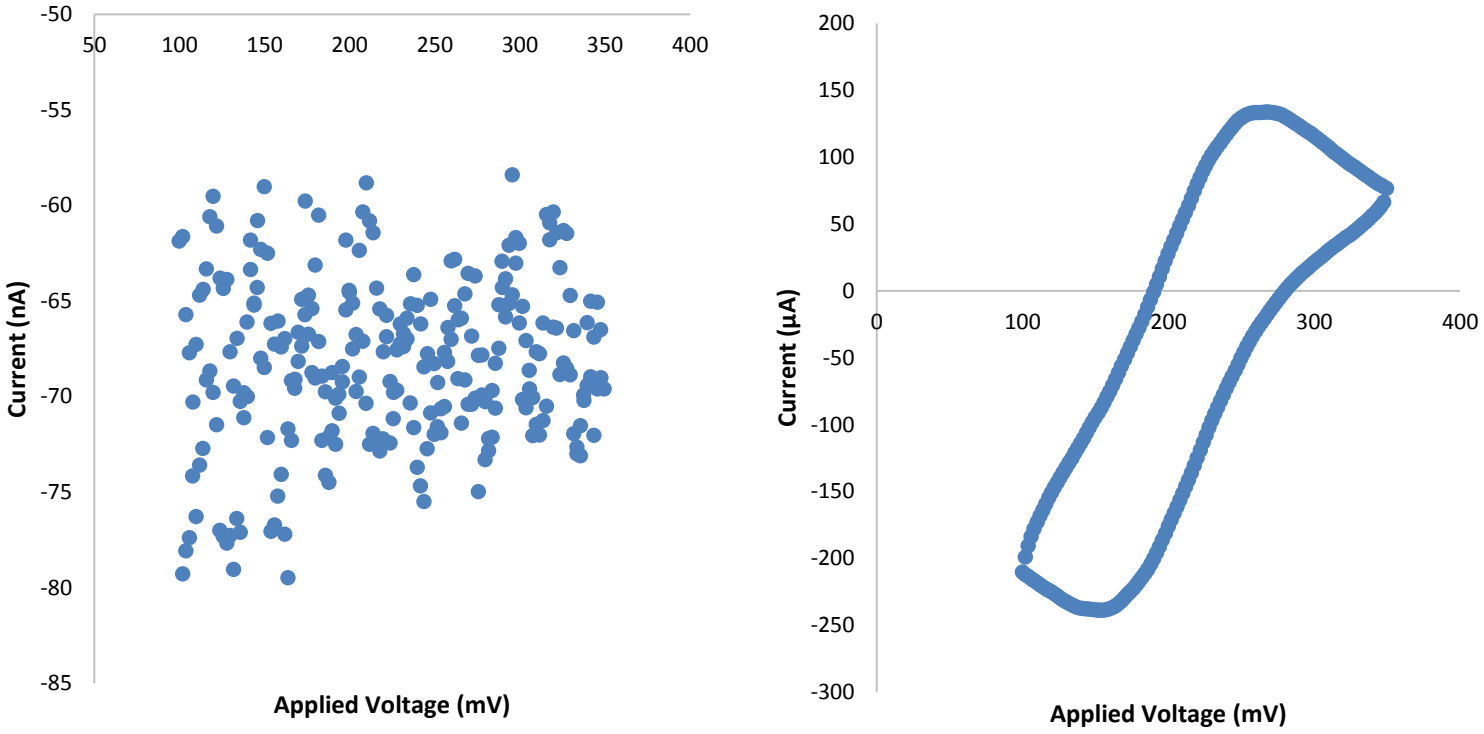

Fig. 8. CV Testing on 4-mercaptobutyric acid SAM before (left) and after (right)

The CV's indicate that the SAM had degraded during the experimentation procedure. The operating conditions such as the type of SAM, frequency range, voltage offset, use of buffers in solution, and nitrogen degassing were varied; however no set of conditions resulted in complete titration curves agreeable with the literature. Below in Fig. 9. A wide range of voltage offsets are tested on a 4 carbon chain carboxylic acid SAM.

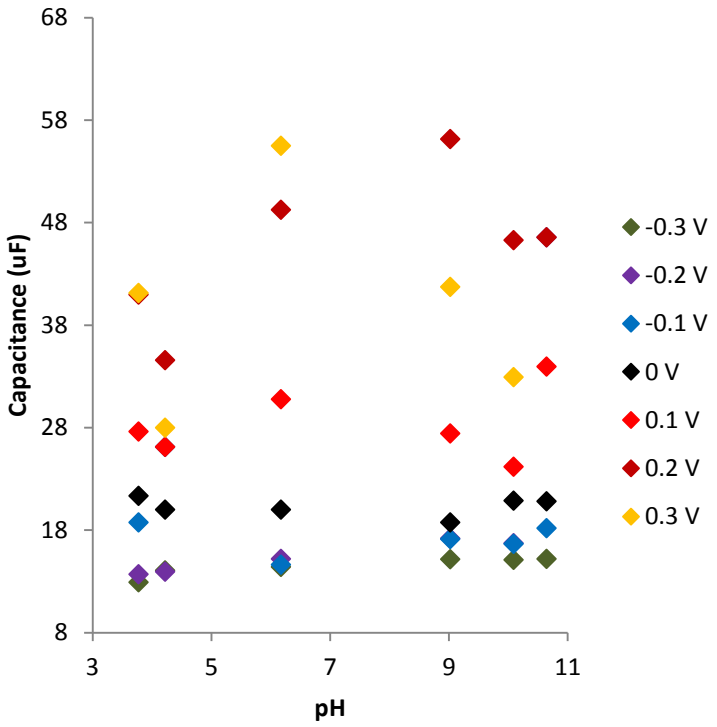

Fig. 9. New 4-mercaptobutyric acid made in TFA tested with HCl, NaOH, NaCl, Stored for 1 day

The collective data of trials indicated: (1) voltage offsets greater than 0.1V result in very high capacitance values, and therefore, these voltage offsets may degrade the SAM, (2) voltage offsets of -0.1, -0.2, and -0.3 result in similar values of capacitance (3) relative standards deviations were generally low (<5%) for trials taken in triplicate, (4) capacitance generally increases with SAM degradation, (5) low frequency ranges tend to degrade SAMs at a lower rate, and (6) the magnitudes of measured capacitance vary between experiments, and therefore SAM quality depends on the atmospheric conditions, such as temperature and pressure, during SAM preparation.

Since no set of operating conditions resulted in complete titration curves for 4-mercaptobutyric acid SAM, we decided to conduct experimentation with a silane adsorbed to an ITO slide. Silanes adsorb to ITO slides more strongly than sulfur adsorbs to gold; therefore we expected less degradation to occur. We conducted experiments using 3-mercaptopropylsilane, which has a high pka, and therefore, is a not an ideal choice of SAM. Nevertheless, use of this SAM was practical because no other acidic silane was available in the laboratory, few acidic silanes were available for purchase, and there was insufficient time to synthesize acidic silanes.

Due to the high pka of 3-mercaptopropylsilane, it was expected for capacitance due to be constant with pH during EIS trials. A variation in capacitance would likely occur closer to the pka of the SAM, which is about 12. The data, however, is useful to characterize the degradation of silane-ITO linkages compared to sulfur-gold linkages. Capacitance vs pH at varying voltage offsets was measured as shown below in Fig. 10.

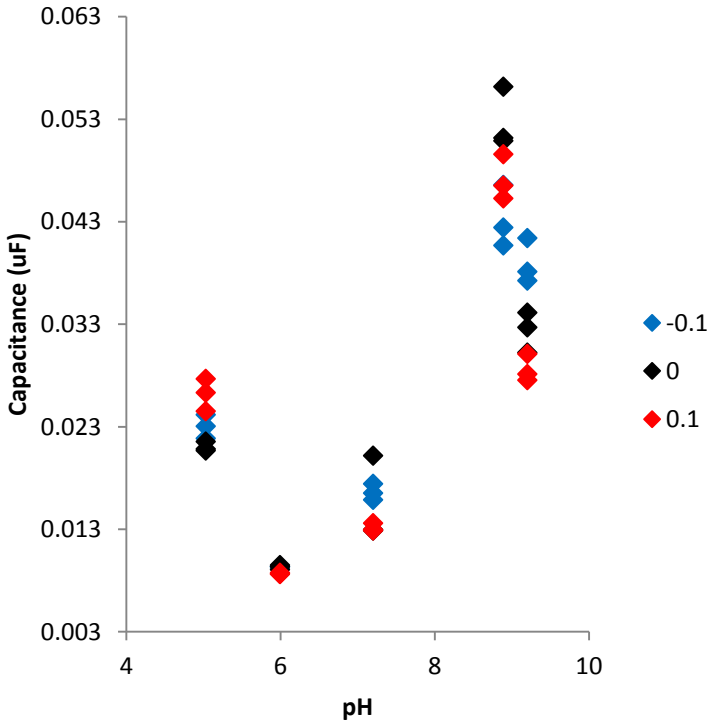

Fig. 10. Si-C3-SH SAM, bubbled with N2, in NaCl, NaOH, NaCl

Each EIS trial resulted in an increase in capacitance regardless of the pH and offset voltage. For instance, the first EIS trial was conducted at a pH of 6 and voltage offset of 0.1V, and the last trial was conducted at a pH of 9 and a voltage offset of 0V. Therefore, we assumed that each measurement caused degradation in the SAM. Degradation was measured with CV's before and after the titration as shown below in Fig. 11.

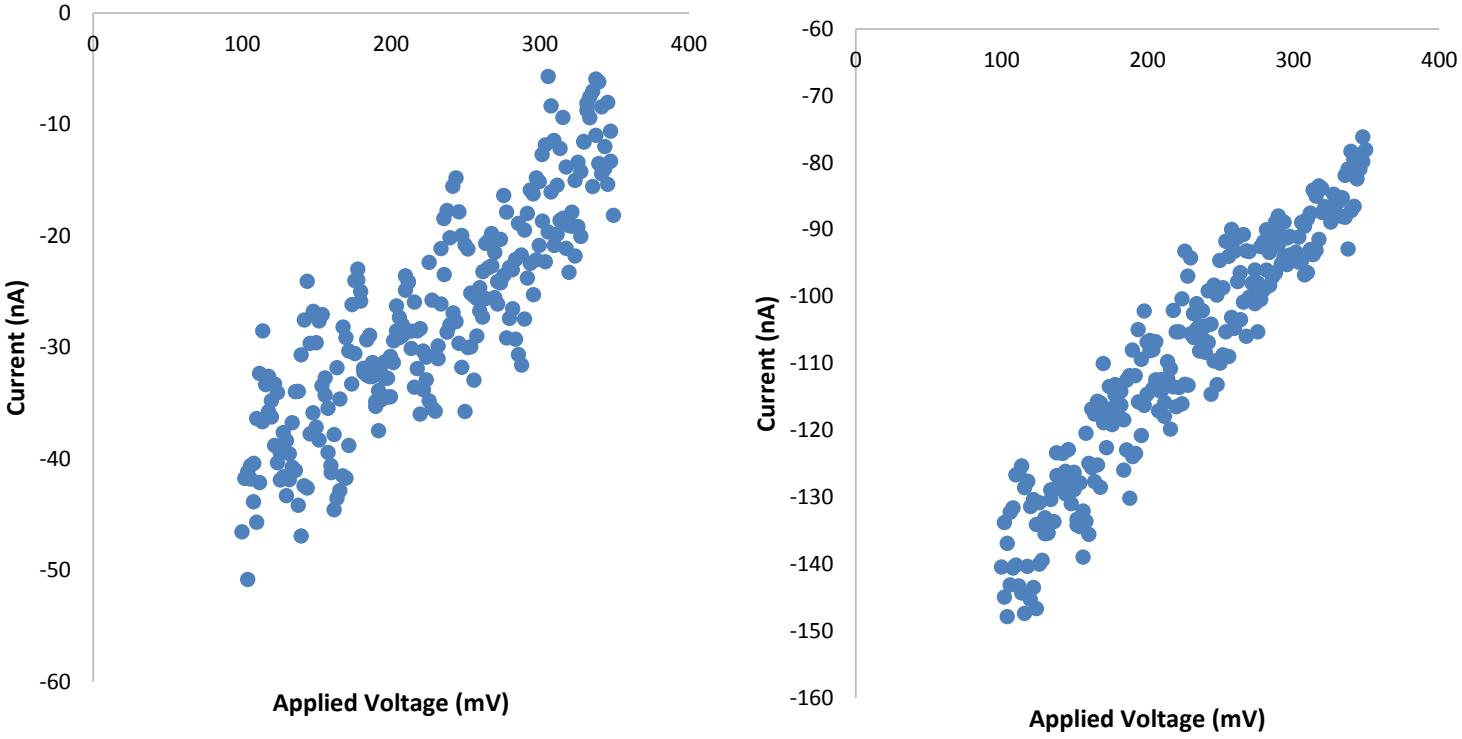

Fig. 11. CV testing on silane-ITO SAM before EIS (left) and after (right).

The CV results indicated that the silane had possibly degraded due to the shift in the scale of the current measurments. We had not expected the EIS trials to degrade the silane SAM. It is possible that the SAM was not well-formed on the ITO substrate due to the short 3-carbon tail. Furthermore, the 3-mercaptopropylsilane was previously stored in the laboratory for an unknown amount of time. It is possible that newly purchased or synthesized SAMs would be more durable for the titration experiments.

Since the experiments with silane did not produce desirable data, we decided to investigate 3-mercapto-1-propane sulfonic acid adsorbed to a gold substrates. This SAM was not necessarily more stable than previously investigated SAMs. Sulfonic acid, however, is most applicable for catalytic studies, and therefore, we deemed that investigation of this SAM would have the greatest impact on future research. First, capacitance vs pH data was measured at various voltage offsets as shown in Fig. 12 below.

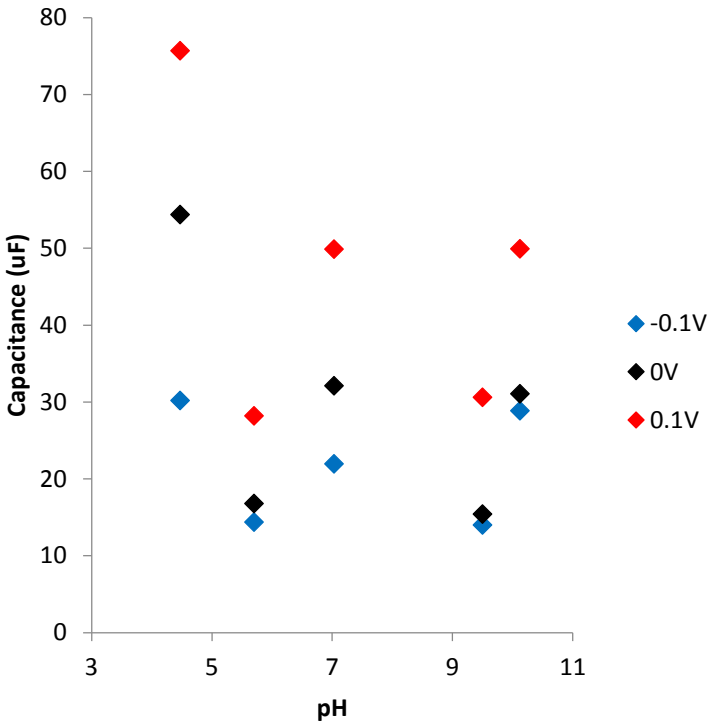

Fig. 12. 3-mercapto-1-propane sulfonic acid SAM, bubbled with N2 in HCl, NaOH, and NaCl

The SAM degraded during the experimental procedure, as indicated by CV's before and titration tests as shown in Fig. 13 below.

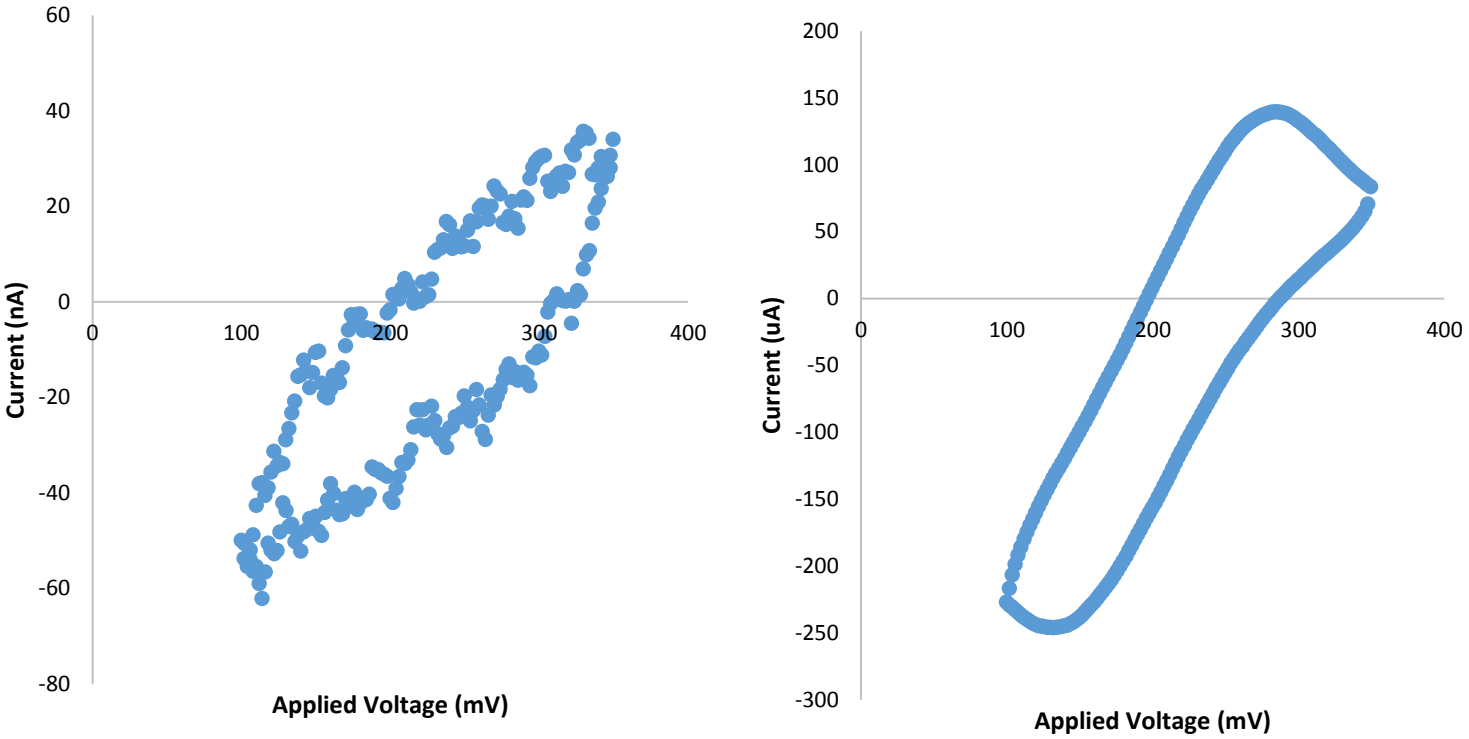

Fig. 13. CV Testing on 3-mercapto-1-propane sulfonic acid SAM before EIS (left) and after (right)

The project then diverged to the investigation of the operating condition(s) that result in SAM degradation and improved SAM stability.

3.2 SAM Stability Tests

SAM stability tests were designed to manipulate one operating condition at a time and to subsequently use CV to measure the resulting SAM degradation. Fig. 14 below presents a CV for a cleaned gold slide without an adsorbed SAM. The difference in height between the oxidation peak and the reduction peak was calculated to be 498 μA; this value represents 100% SAM degradation. We assumed that SAM degradation was proportional to the difference in height between the oxidation and reduction peaks to quantify degradation. Percent degradation was calculated by dividing difference in peak height by the difference in height of pure gold.

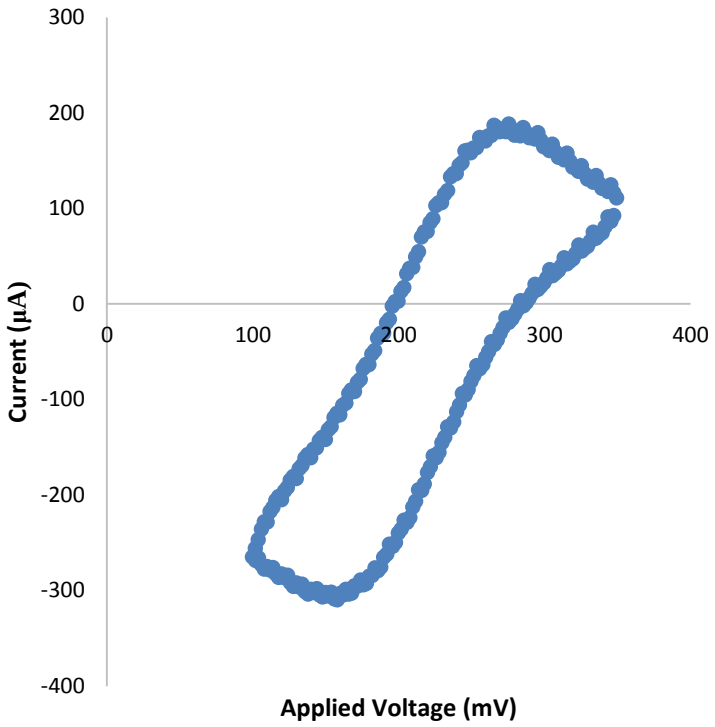

Fig. 14. CV of Cleaned Gold Slide

We then defined normal operating conditions which are shown below in Table 1. These operating conditions were chosen because they were thought to be the least degrading. We aimed to vary one operating condition at a time while avoiding degradation from all other operating conditions.

Table 1. Standard operating conditions for stability tests.

Operating Condition	Value
Upper Frequency Limit	100,000 Hz
Lower Frequency Limit	3 Hz
Offset Voltage	0 V
Perturbation Voltage	5 mV
pH	7
SAM solvent	Ethanol
Storage Time	0 Days

We measured the data from one CV, five EIS trials at normal operating conditions, and another CV following EIS. The CV results are shown in Fig. 15 below.

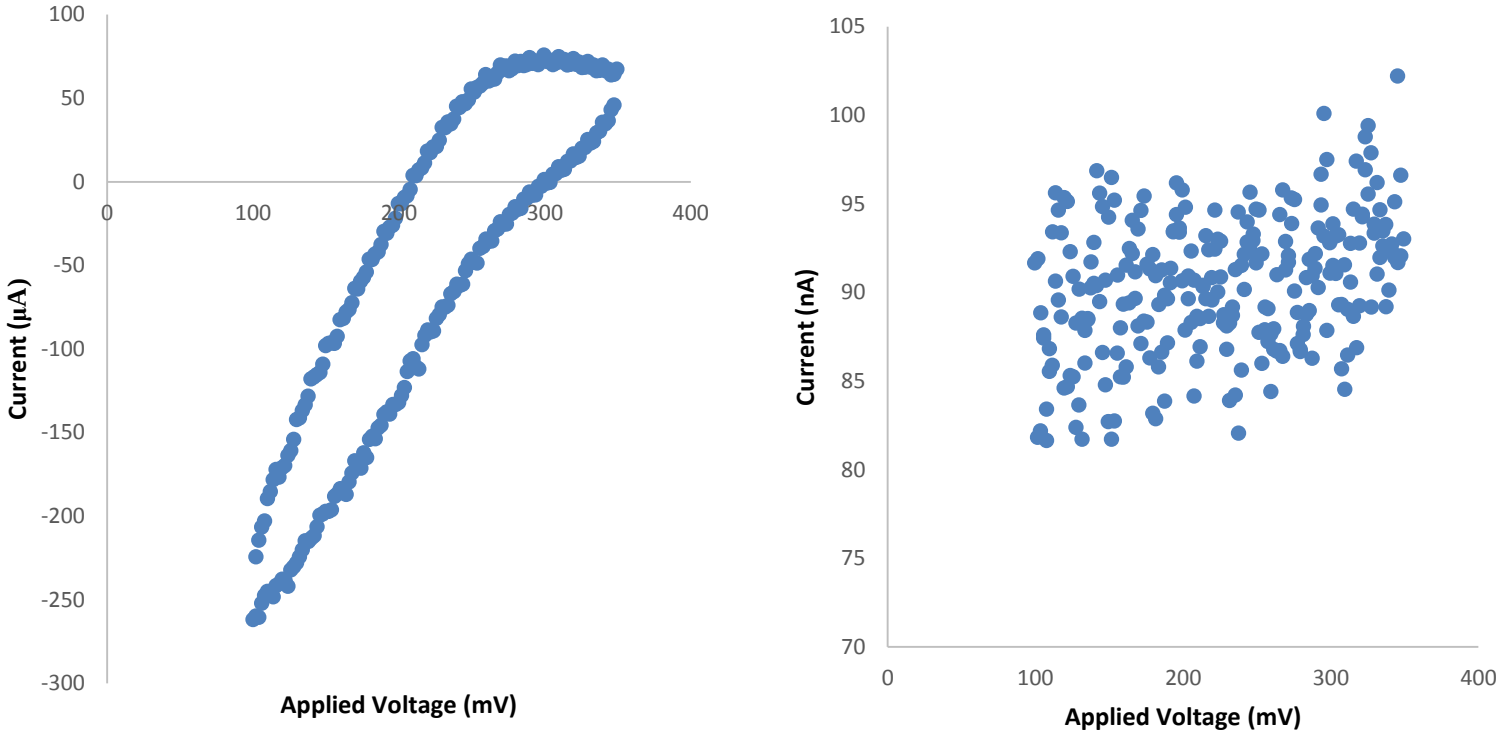

Fig. 15. CV After Testing Standard Conditions

The results indicate that the normal operating conditions, which were thought to be the least degrading, resulted in 84% SAM degradation. Therefore, conditions such as backfilling electrodes, increasing nitrogen degassing times, increasing the frequency lower limit, and changing the SAM solution solvent were conducted to increase SAM stability. Furthermore, common experimental norms were investigated such as the storage duration after extraction from SAM solvent, and the atmospheric exposure after extraction from SAM solvent.

The results from stability testing are shown below in Table 2. For each category two to three different operating conditions are shown. We determined that each set of operating conditions either result in a great amount of SAM degradation (>80%) or virtually no SAM degradation (<0.1%). In Table 2, a red operating condition consistently lead to SAM degradation. A yellow operating condition lead to SAM degradation in some instances but preserved SAM

quality in others. Alliteratively, a yellow condition had no positive or negative effect. Green operating conditions consistently preserved SAM quality and are therefore recommended for titration tests. It should be noted that it was difficult to attribute degradation to specific conditions. Storage duration and atmospheric exposure, for instance, are difficult to keep constant between trials. Also, few sample sizes were conducted for each set of operating conditions. Therefore, the Table 2 was constructed to best represent our accumulation of data; Table 2 should not be considered definitive.

Table 2. 3-mercapto-1-propanesulfonate SAM stability test results.

Frequency Lower Range	0.1Hz	3 Hz	N/A
Backfilling	Unbackfilled	8-carbon tail	N/A
SAM Solvent	Methanol	Ethanol	N/A
Storage Duration	Instant	1 day	2 day
Atmospheric Exposure	15 minutes	3 hours	N/A
Degassing	30 minutes	1 hour	N/A

Additionally we thought that turning off the Gamry Reference 600 or changing the Gamry Framework software while a gold slide was attached may degrade the SAM; however experiments showed that this was not the case. Furthermore, we conducted a series of 30 CV's on a SAM; and little degradation occurred. It is possible that the SAM degradation occurs upon its transfer between solutions. We believe that the carboxylic acid SAMs were more stable than the sulfonic acid SAMs from the experimentation performed. Stability tests were not performed on the carboxylic acid SAMs; however the pH titration tests indicated that the carboxylic SAMs may have been more stable. This could be due to the lower solubility of carboxylic acid in water. Also, since these SAMs contained four carbons, they likely produced more well-ordered films.

4.0 Conclusions

We attempted to measure the effect of voltage on pk_a for solid acid catalysts. We determined that SAM degradation hinders the measurement of potential-driven SAM protonation and deprotonation. The experimental conditions resulted in SAM degradation after some amount of EIS experiments were performed. Consequently, the project diverged to the investigation of factors that lead to SAM degradation. A variety of factors result in SAM degradation; the most degrading factors included, atmospheric exposure, presence of dissolved oxygen, and low frequency limits. Some factors degraded SAMs without electrochemical testing, such as storage times and atmospheric exposure. Therefore synthesizing SAMs with consistently high quality is a priority. Chain lengths greater than three carbons and strong substrate/head-group bonds such as silanes to ITO electrodes may help improve SAM quality and resistance to destructive conditions. We recommend the use of silanes with 4-carbon chain lengths. Also, we recommend conducting titration tests in a ferricynaide solution to reduce degassing times; though this will reuire the determination of reduction-oxidation potential as a function of pH. Ultimately, voltage-induced pk_a variation will allow researchers to determine the precise pk_a that converts biomass to glucose.

Acknowledgements

Thank you to Professor Timko and Professor Lambert for their advice and support throughout the duration of this MQP. Their guidance was imperative for our progression with this project and our findings in this report. Also, thank you to Aung Lynn and Anthony Salerni for their assistance with SAM preparation techniques and electrochemical testing.

References

Andreu, Rafael, and W. Ronald Fawcett. "Discreteness-of-Charge Effects at Molecular Films Containing Acid/Base Groups." *The Journal of Physical Chemistry* 98, no. 48 (December 1, 1994): 12753–58. doi:10.1021/j100099a045.

Ashwell, Geoffrey J., Marta Sujka, and Andrew Green. "Molecular Rectification: Stabilised Alignment of Chevron-Shaped Dyes in Hybrid SAM/LB Structures in Which the Self-Assembled Monolayer Is Anionic and the Langmuir–Blodgett Layer Is Cationic." *Faraday Discuss.* 131 (2006): 23–31. doi:10.1039/B505785J.

Bryant, Mark A., and Richard M. Crooks. "Determination of Surface pKa Values of Surface-Confined Molecules Derivatized with pH-Sensitive Pendant Groups." *Langmuir* 9, no. 2 (February 1, 1993): 385–87. doi:10.1021/la00026a005.

Burgess, Ian, Brian Seivewright, and R. Bruce Lennox. "Electric Field Driven Protonation/Deprotonation of Self-Assembled Monolayers of Acid-Terminated Thiols." *Langmuir* 22, no. 9 (April 1, 2006): 4420–28. doi:10.1021/la052767g.

Cao, Xiao-Wei. "Study of Electrode Potential Effect on Acid–base Behavior of ω-Functionalized Self-Assembled Monolayers Using Fourier Transform Surface-Enhanced Raman Scattering Spectroscopy." *Journal of Raman Spectroscopy* 36, no. 3 (March 1, 2005): 250–56. doi:10.1002/jrs.1298.

Dai, Zong, and Huangxian Ju. "Effect of Chain Length on the Surface Properties of ω-Carboxy Alkanethiol Self-Assembled Monolayers." *Physical Chemistry Chemical Physics* 3, no. 17 (2001): 3769–73. doi:10.1039/b104570a.

Fawcett, W. Ronald, Milan Fedurco, and Zuzana Kovacova. "Double Layer Effects at Molecular Films Containing Acid/Base Groups." *Langmuir* 10, no. 7 (July 1, 1994): 2403–8. doi:10.1021/la00019a062.

González-Granados, Zoilo, Guadalupe Sánchez-Obrero, Rafael Madueño, José M. Sevilla, Manuel Blázquez, and Teresa Pineda. "Formation of Mixed Monolayers from 11-Mercaptoundecanoic Acid and Octanethiol on Au(111) Single Crystal Electrode under Electrochemical Control." *The Journal of Physical Chemistry C* 117, no. 46 (November 21, 2013): 24307–16. doi:10.1021/jp406229f.

Hvolbæk, Britt, Ton V. W. Janssens, Bjerne S. Clausen, Hanne Falsig, Claus H. Christensen, and Jens K. Nørskov. “Catalytic Activity of Au Nanoparticles.” *Nano Today* 2, no. 4 (August 2007): 14–18. doi:10.1016/S1748-0132(07)70113-5.

Kakiuchi, Takashi, Minehiko Iida, Shin-ichiro Imabayashi, and Katsumi Niki. “Double-Layer-Capacitance Titration of Self-Assembled Monolayers of ω-Functionalized Alkanethiols on Au(111) Surface.” *Langmuir* 16, no. 12 (June 1, 2000): 5397–5401. doi:10.1021/la991358f.

Love, J. Christopher, Lara A. Estroff, Jennah K. Kriebel, Ralph G. Nuzzo, and George M. Whitesides. “Self-Assembled Monolayers of Thiolates on Metals as a Form of Nanotechnology.” *Chemical Reviews* 105, no. 4 (April 1, 2005): 1103–70. doi:10.1021/cr0300789.

Milkani, Eftim. "Modification of Surfaces for Biological Applications." PhD diss., Worcester Polytechnic Institute, 2010.

Raj, C. Retna, and S. Behera. “Electrochemical Studies of 6-Mercaptonicotinic Acid Monolayer on Au Electrode.” *Journal of Electroanalytical Chemistry* 581, no. 1 (July 15, 2005): 61–69. doi:10.1016/j.jelechem.2005.04.012.

Schweiss, Ruediger, Carsten Werner, and Wolfgang Knoll. “Impedance Spectroscopy Studies of Interfacial Acid–base Reactions of Self-Assembled Monolayers.” *Journal of Electroanalytical Chemistry* 540 (January 2, 2003): 145–51. doi:10.1016/S0022-0728(02)01303-7.

Smith, C. P., and H. S. White. “Voltammetry of Molecular Films Containing Acid/base Groups.” *Langmuir* 9, no. 1 (January 1, 1993): 1–3. doi:10.1021/la00025a001.

Smith, Rachel K, Penelope A Lewis, and Paul S Weiss. “Patterning Self-Assembled Monolayers.” *Progress in Surface Science* 75, no. 1–2 (June 2004): 1–68. doi:10.1016/j.progsurf.2003.12.001.

Sugihara, Kouki, Katsuaki Shimazu, and Kohei Uosaki. “Electrode Potential Effect on the Surface pKa of a Self-Assembled 15-Mercaptohexadecanoic Acid Monolayer on a Gold/Quartz Crystal Microbalance Electrode.” *Langmuir* 16, no. 18 (September 1, 2000): 7101–5. doi:10.1021/la991301t.

White, Henry S., Jeffery D. Peterson, Qizhi Cui, and Keith J. Stevenson. “Voltammetric Measurement of Interfacial Acid/Base Reactions.” *The Journal of Physical Chemistry B* 102, no. 16 (April 1, 1998): 2930–34. doi:10.1021/jp980035+.

Appendix

Appendix A: 11-mercaptoundecanoic acid

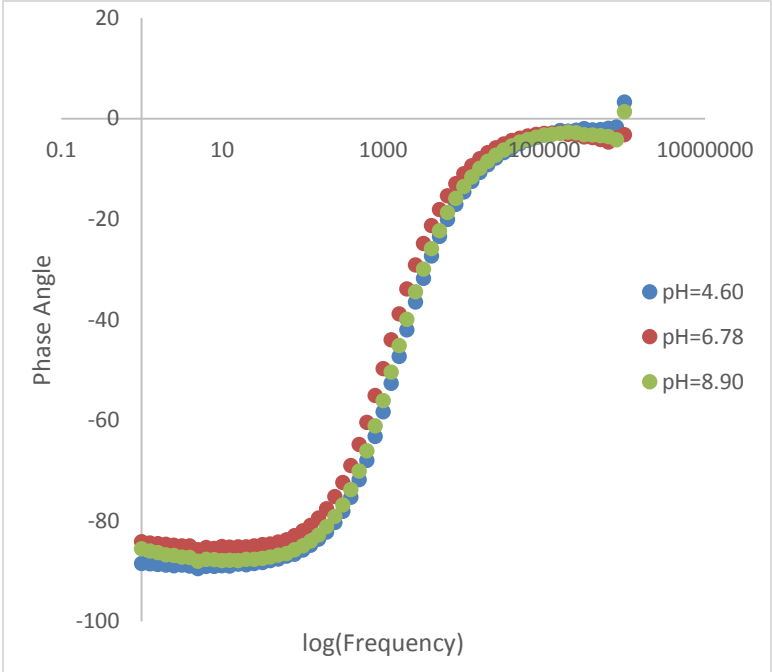

Fig. 16: The Phase Angle versus log(Frequency) response curves for different pH levels at 0V offset.

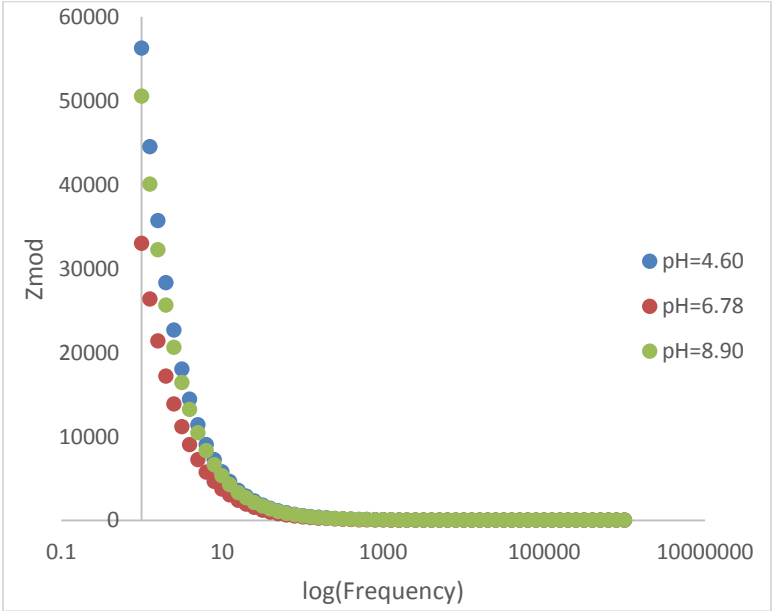

Fig. 17: The Zmod versus log(Frequency) response curves for different pH levels at 0Voffset.

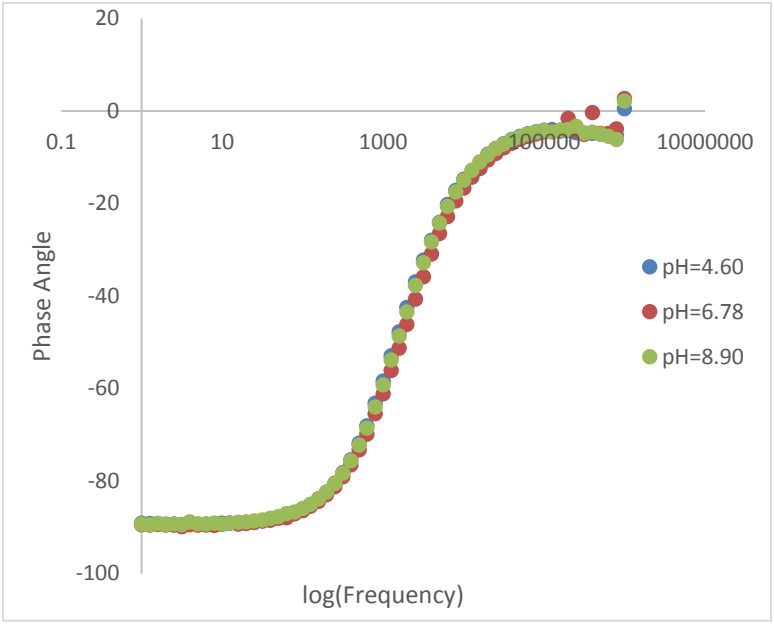

Fig. 18: The Phase Angle versus log(Frequency) response curves at 0V offset

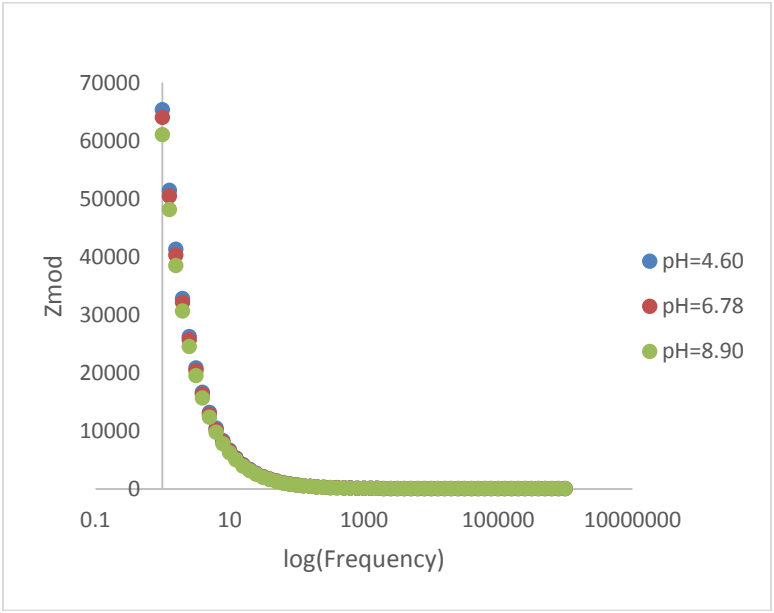

Fig. 19: The Zmod versus log(Frequency) response curves at 0V offset

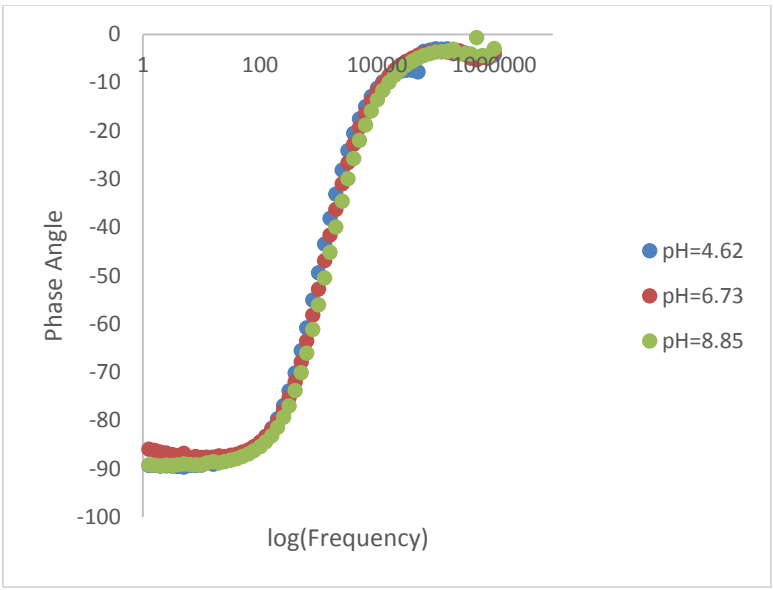

Fig. 20: 0.1 V The Phase Angle versus log(Frequency) response curves at 0.1V offset

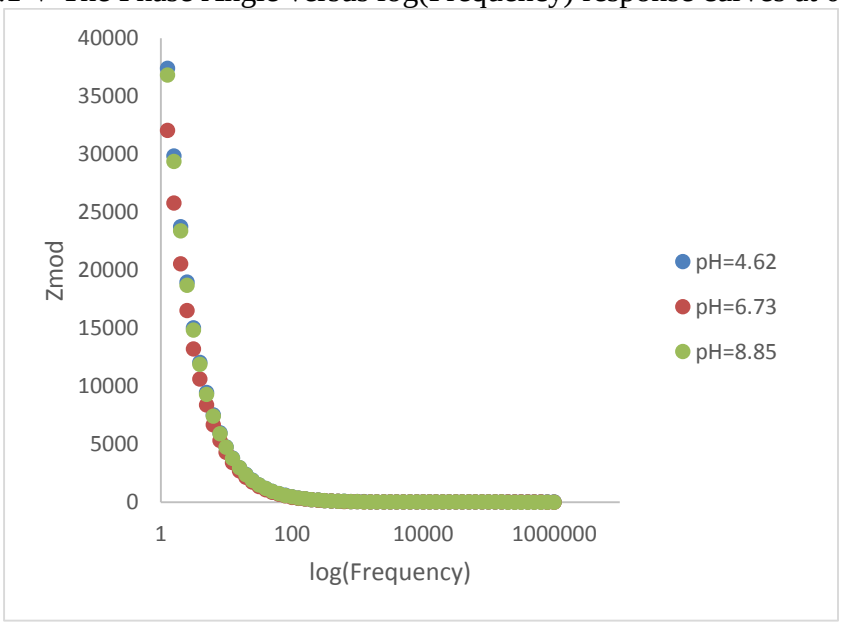

Fig. 21: The Zmod versus log(Frequency) response curves at 0.1V offset

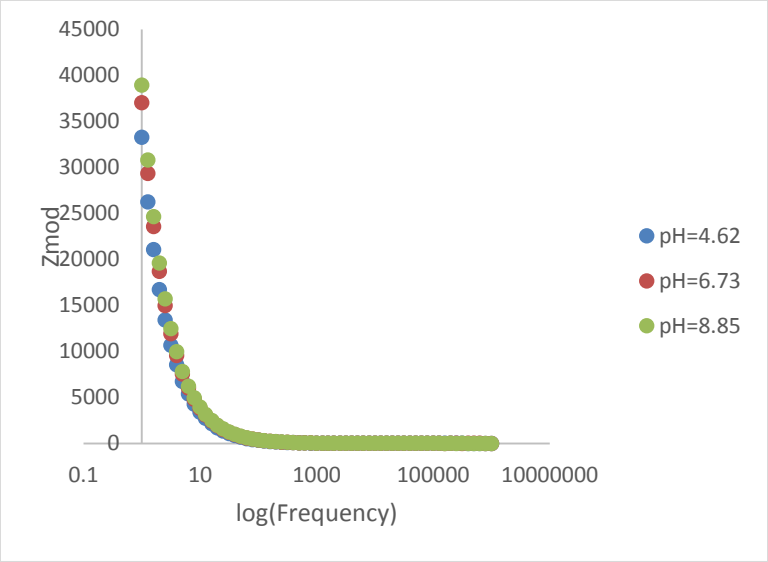

Fig. 22: The Zmod versus log(Frequency) response curves at -0.1V offset

Appendix B: 3-mercaptopropanoic acid

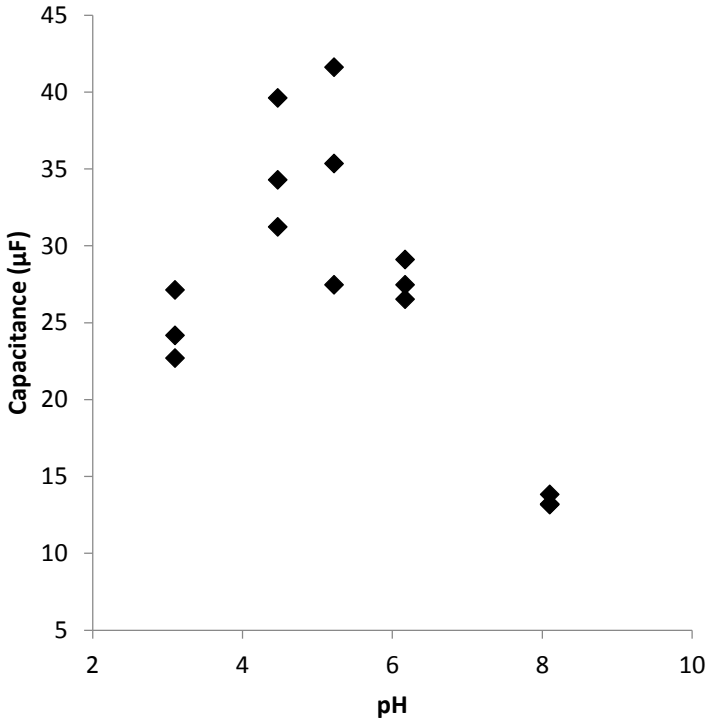

Fig. 23. 3-mercaptopropanoic acid SAM made in ethanol with TFA tested at 0V in citrate buffer

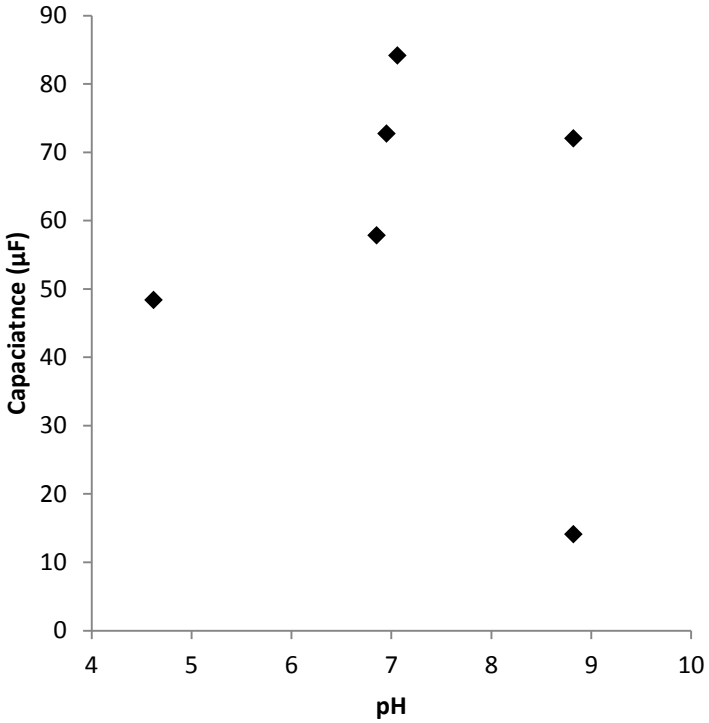

Fig. 24. 3-mercaptopropanoic acid SAM tested in HCl, NaOH, NaCl

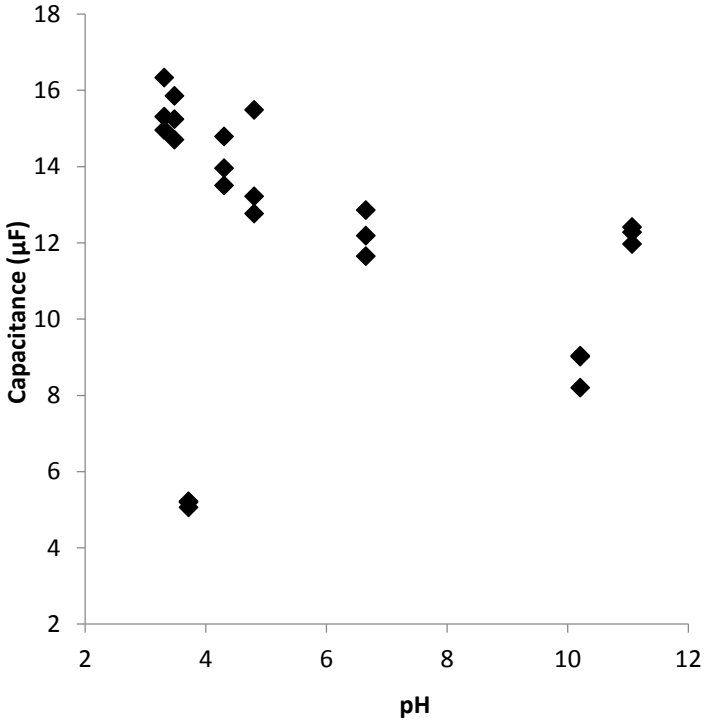

Fig. 25. 3-mercaptopropanic acid made in TFA backfilled with 1-octanehiol tested in HCl, NaOH, NaCl

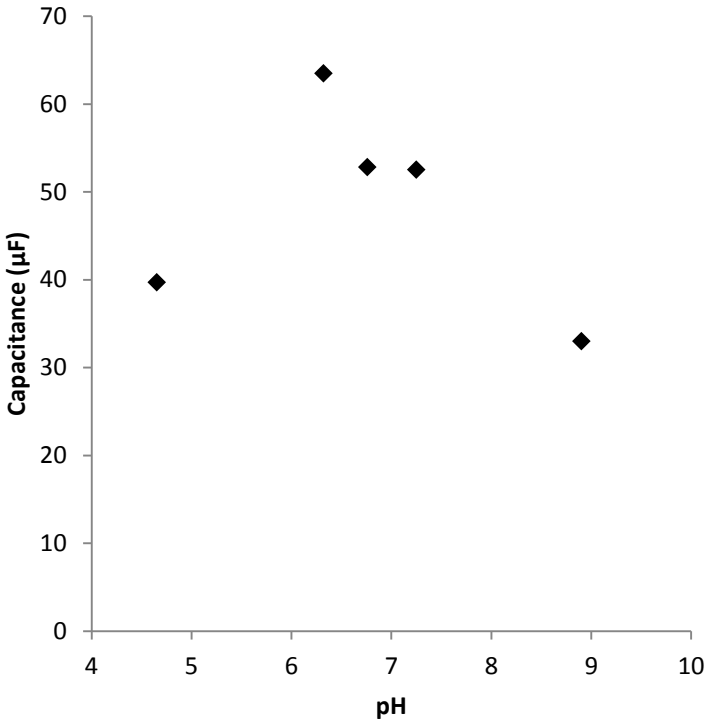

Fig. 26. 3-mercaptopropanic acid tested in HCl, NaOH, NaCl

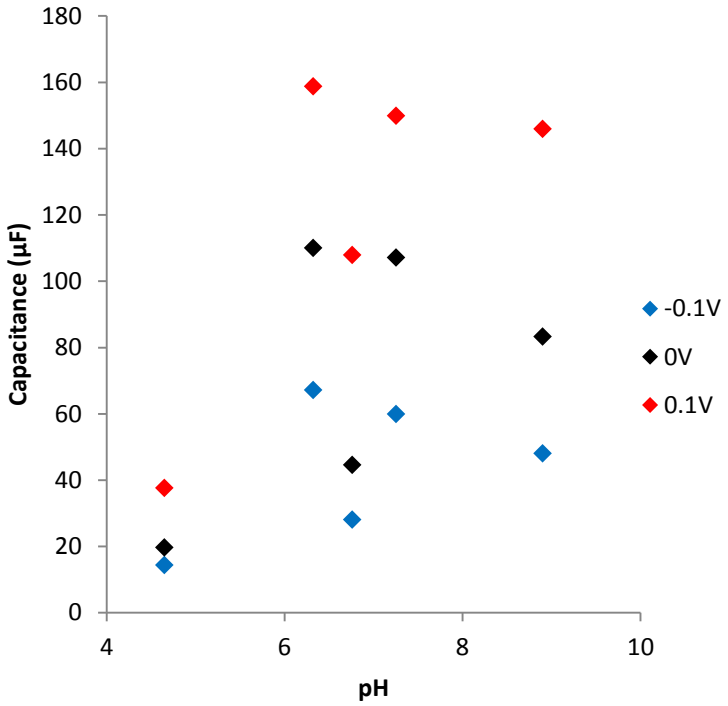

Fig. 27. 3-mercaptopropanic acid tested in HCl, NaOH, NaCl

Appendix C: 4-mercaptobutyric acid

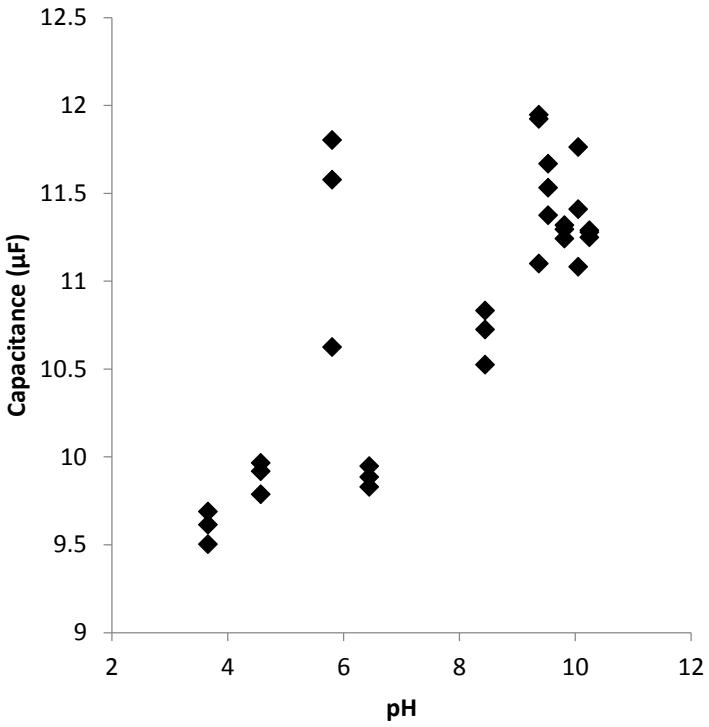

Fig. 28. 4-mercaptobutyric acid SAM made in ethanol with TFA tested at 0V in HCl, NaOH, NaCl

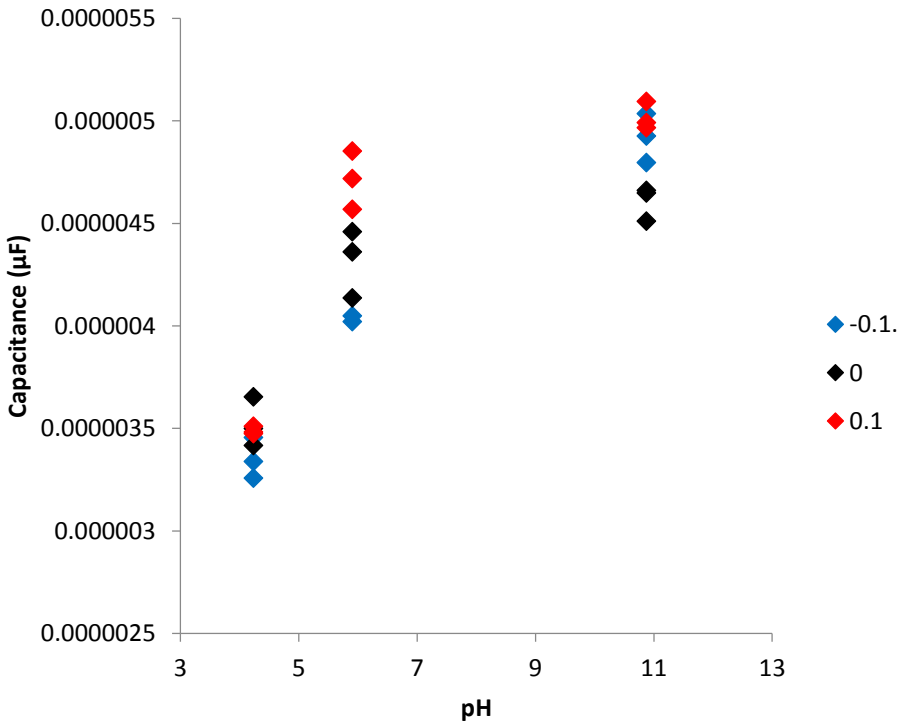

Fig. 29. 4-mercaptobuyric acid made in TFA backfilled with 1-octanethiol tested in HCl, NaOH, NaCl

Appendix D: New 4-mercaptobutyric acid

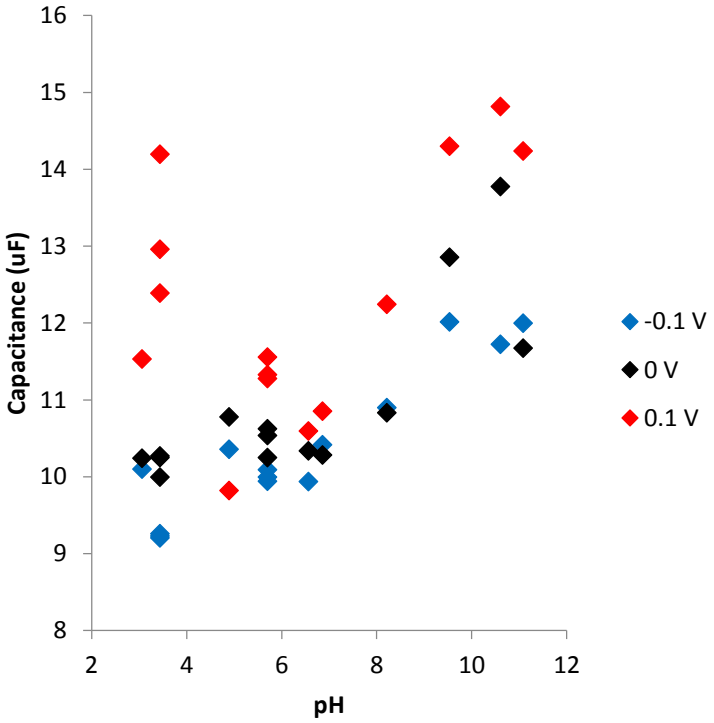

Fig. 30. New 4-mercaptobutyric acid made in TFA tested with HCl, NaOH, NaCl

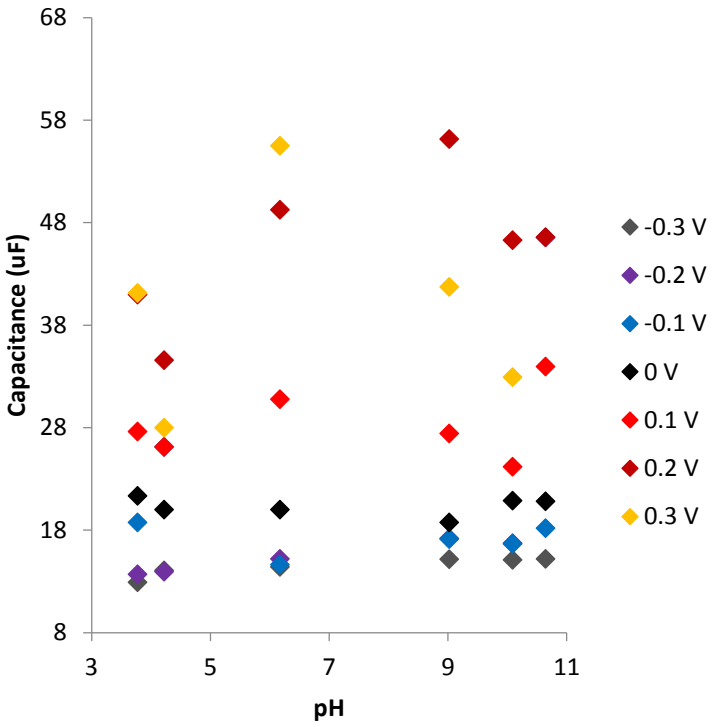

Fig. 31. New 4-mercaptobutyric acid made in TFA tested with HCl, NaOH, NaCl, Store for 1 day

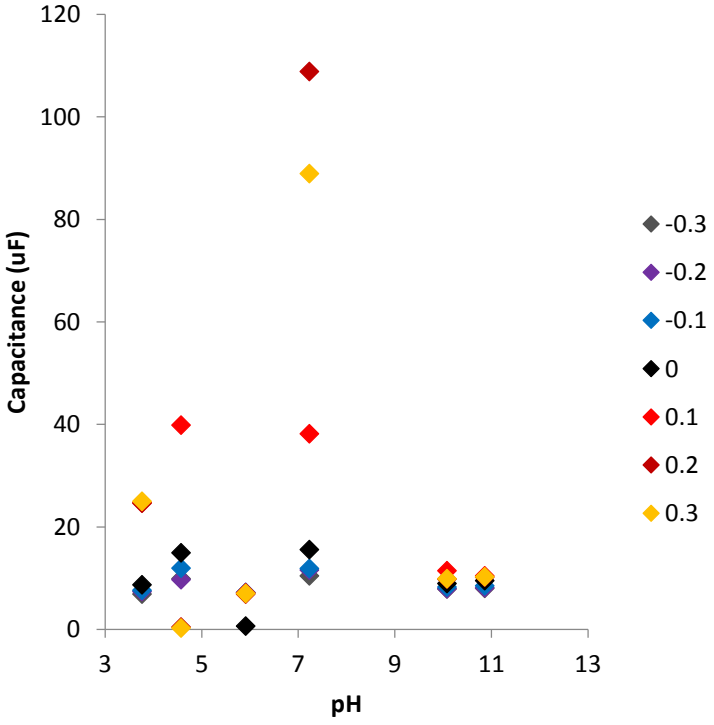

Fig. 32. New 4-mercaptobutyric acid made in TFA tested with HCl, NaOH, NaCl, Stored for 2 days

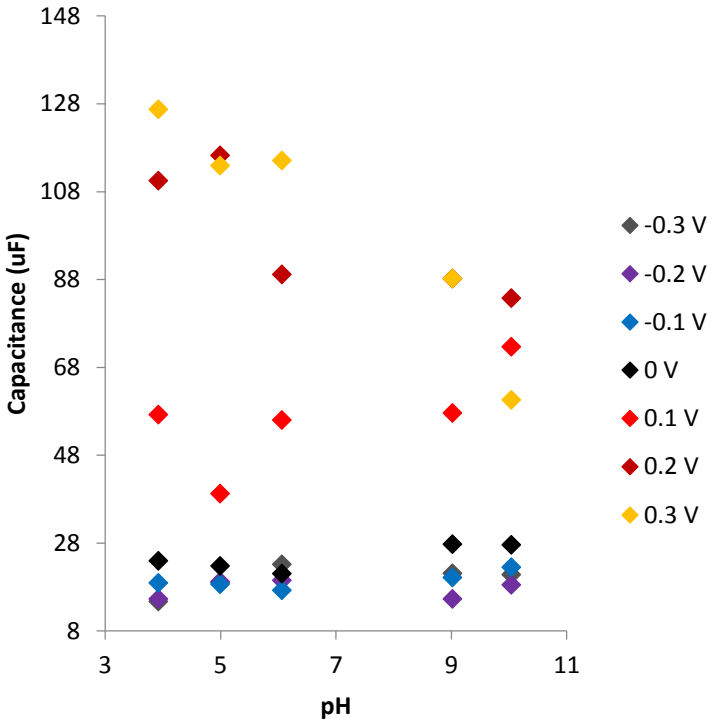

Fig. 33. New 4-mercaptobutyric acid made in TFA tested with HCl, NaOH, NaCl

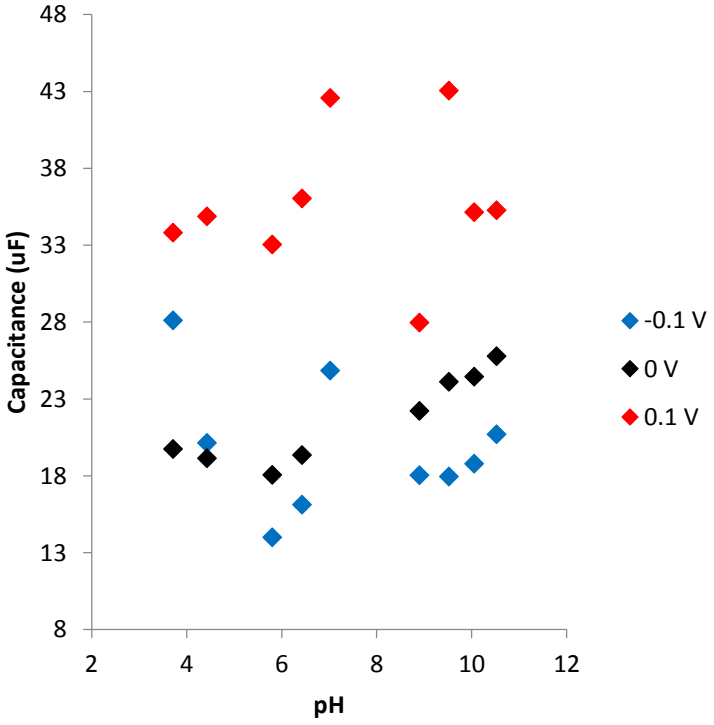

Fig. 34. New 4-mercaptobutyric acid made in TFA tested with HCl, NaOH, NaCl, and Backfilled with 1-ocanethiol and CV tested beforehand

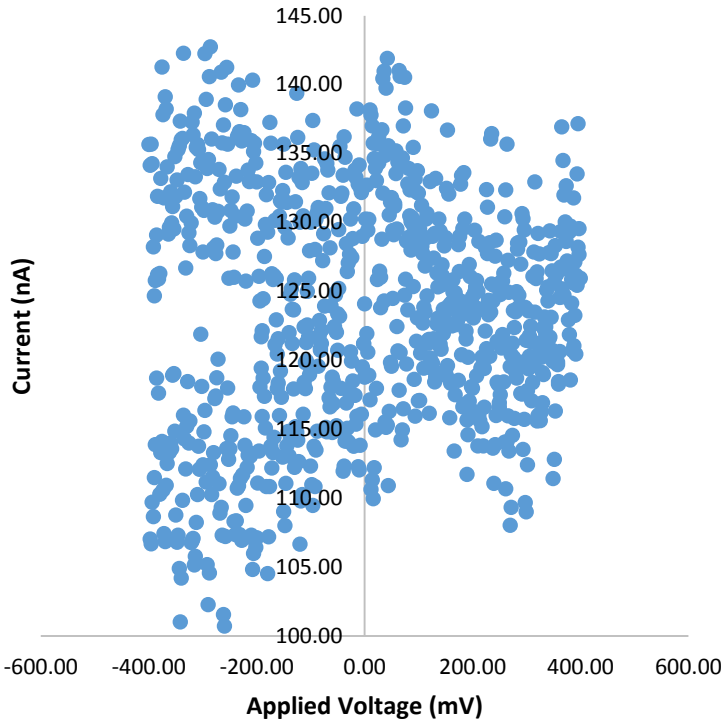

Fig. 35. CV Before Experimentation for above titration curve

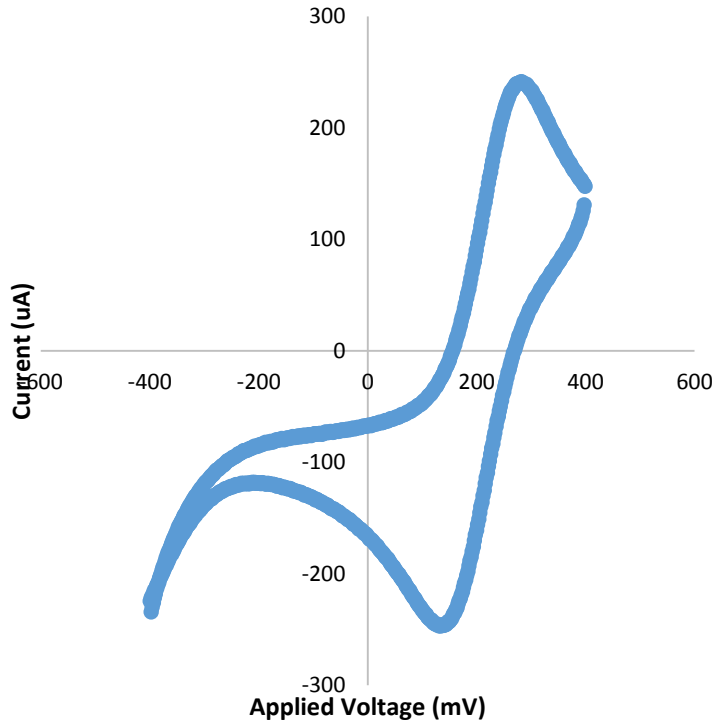

Fig. 36. CV After Experimentation for above titration curve

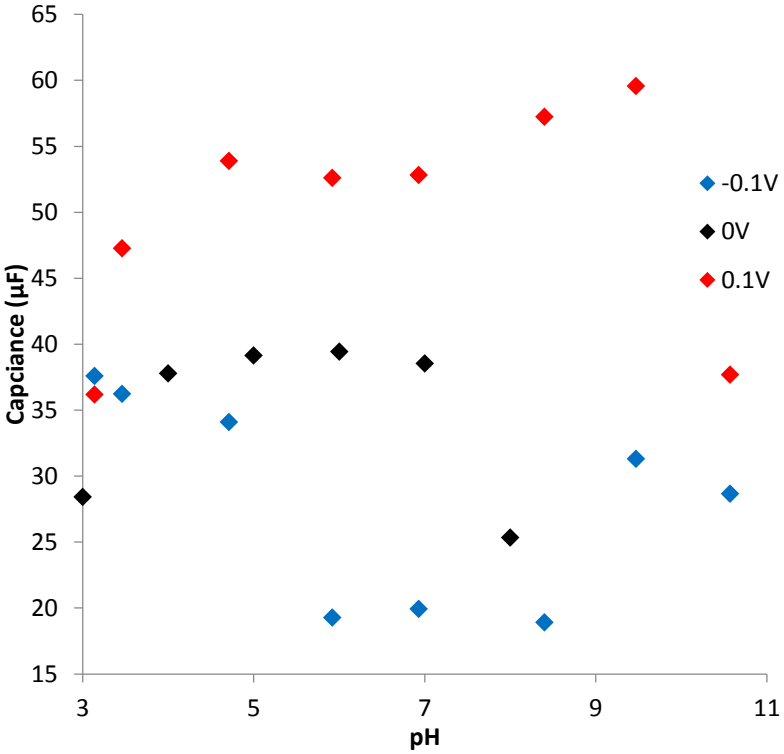

Fig. 37. 4-mercaptobutyric acid made without TFA tested in HCl, NaOH, NaCL, Bubbled with N2

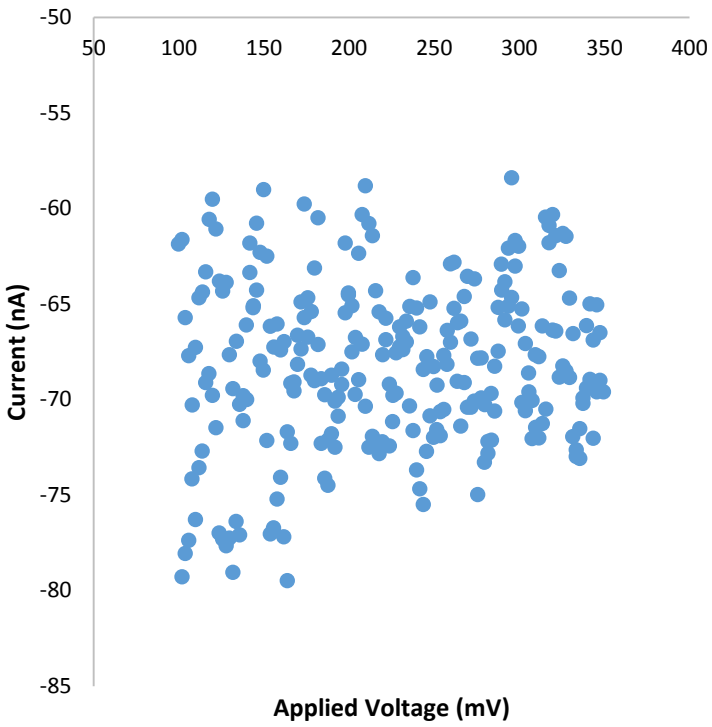

Fig. 38. CV Before Testing for above titration curve

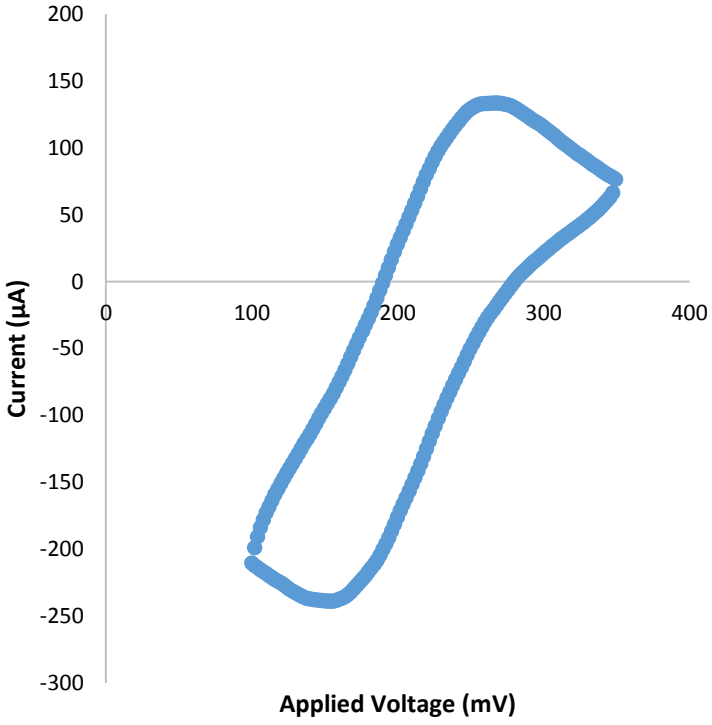

Fig. 39. CV After Testing for above titration curve

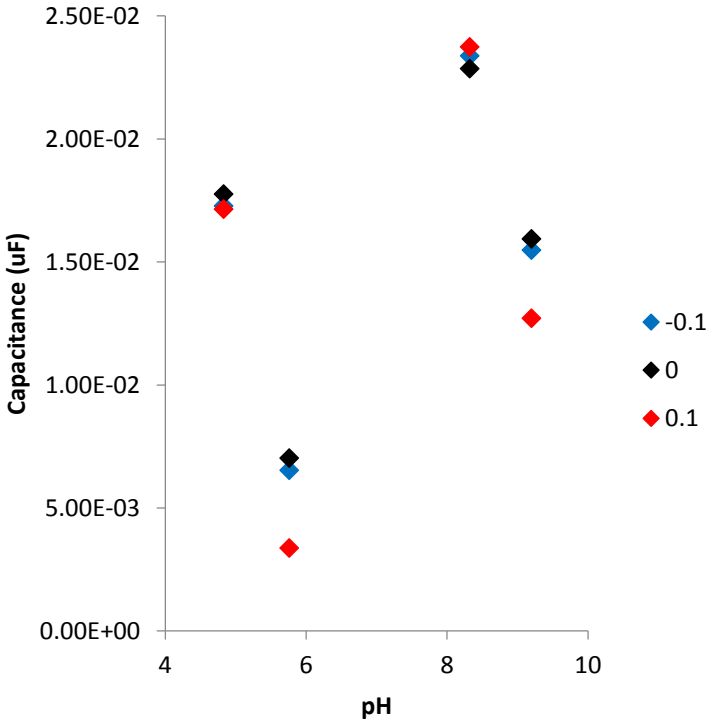

Fig. 40. 4-mercaptobutyric acid SAM made without TFA

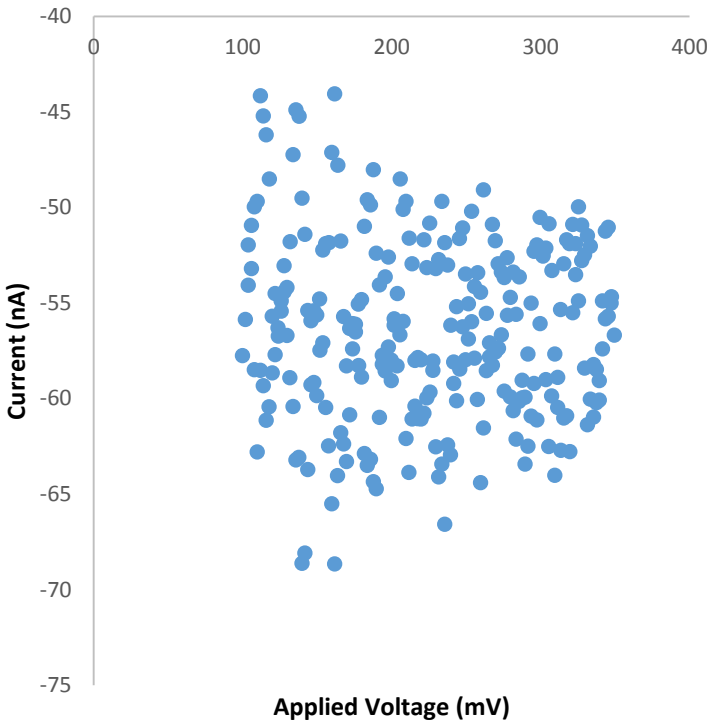

Fig. 41. CV Before Testing for above titration curve

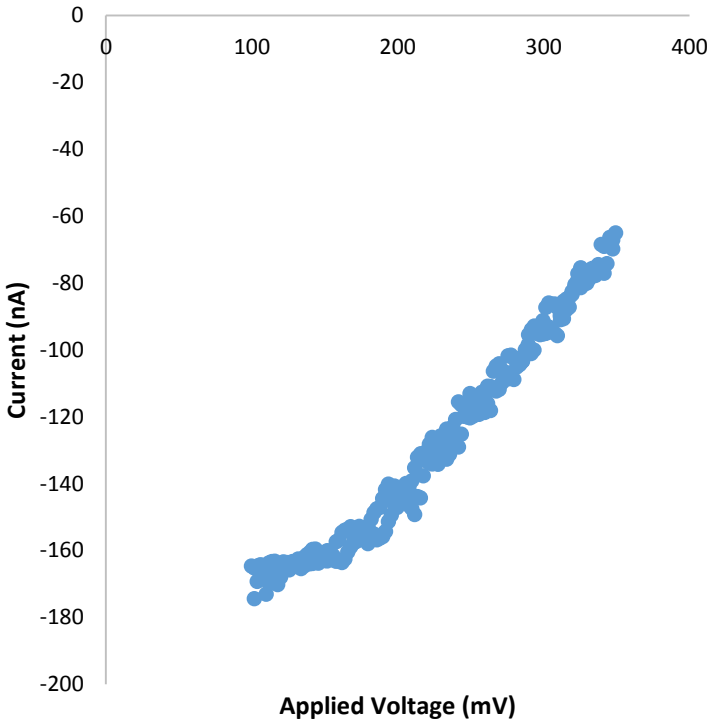

Fig. 42. CV After Testing for above titration curve

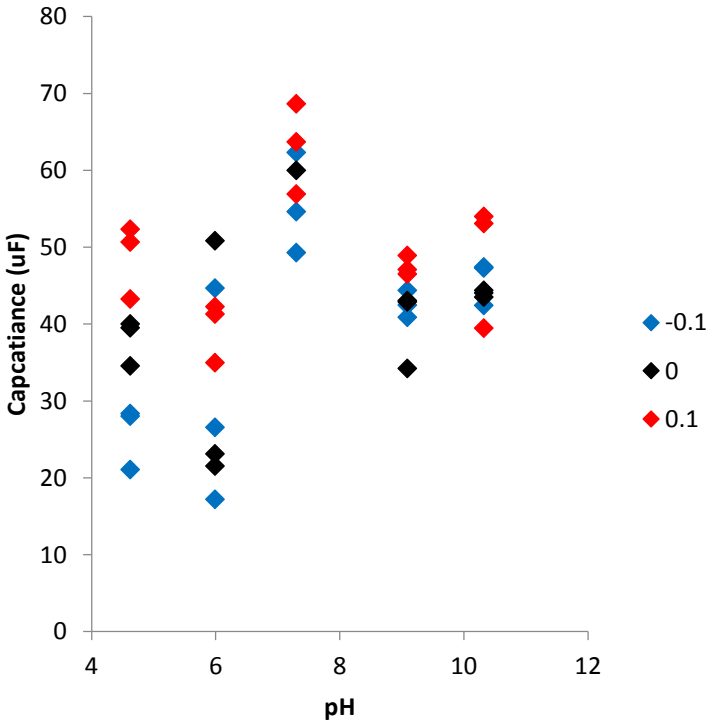

Fig. 43. 4-mercaptobutyric acid SAM made without TFA from same batch as above

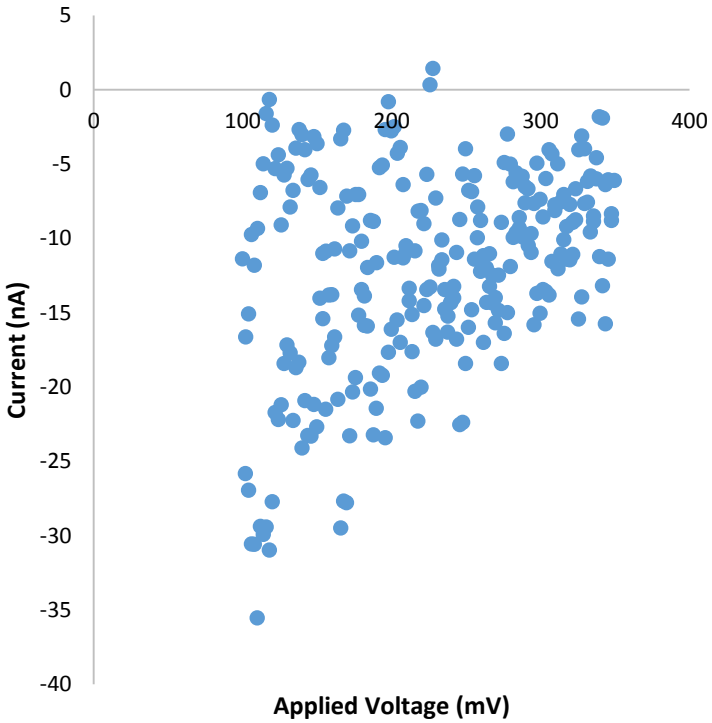

Fig. 44. CV Before Testing for above titration curve

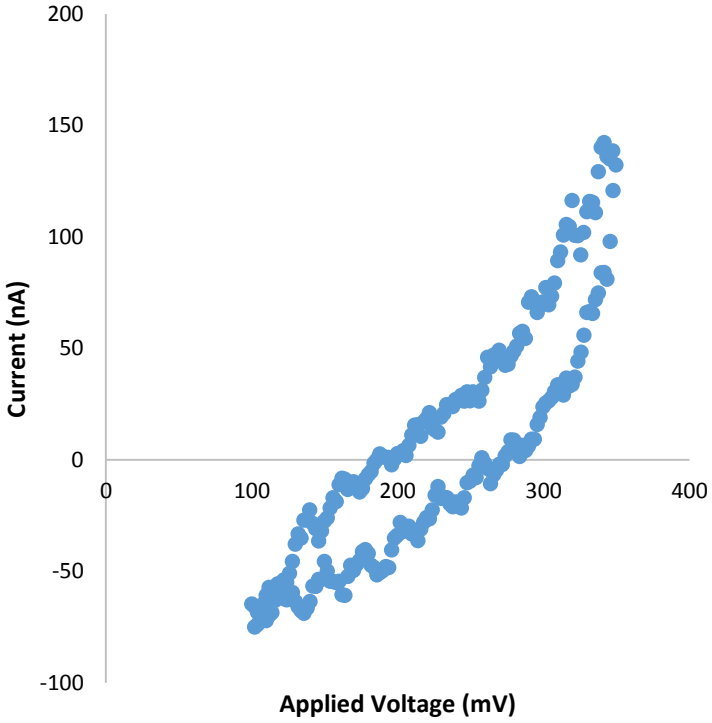

Fig. 45. CV After Testing for above titration curve

Appendix E: 3-mercaptopropylsilane

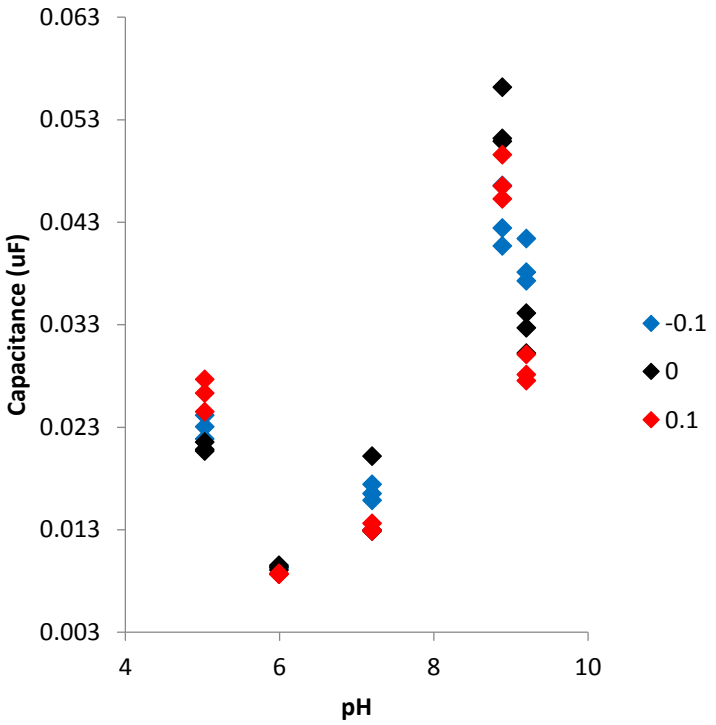

Fig. 46. Si-C3-SH SAM made with lab procedure, bubbled with N2, NaCl, NaOH, NaCl

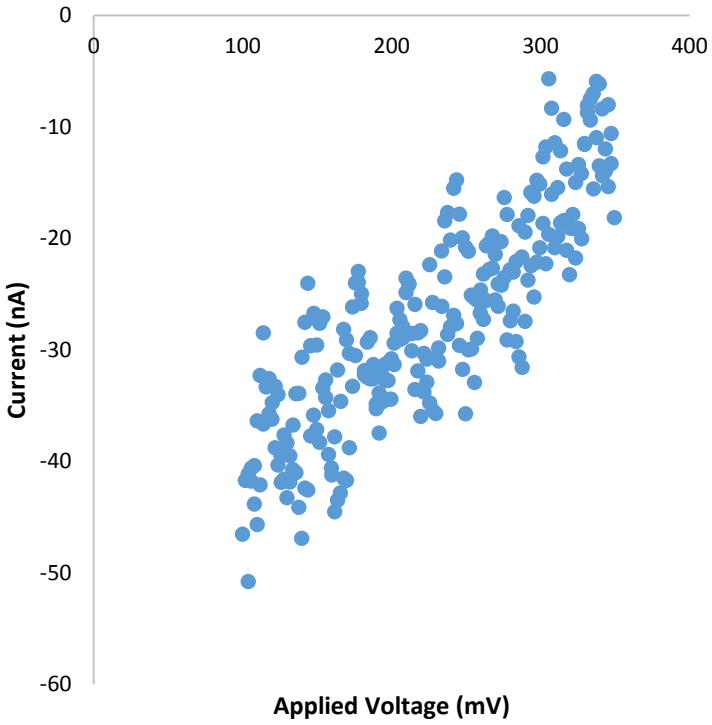

Fig. 47. CV Before Testing for above titration curve

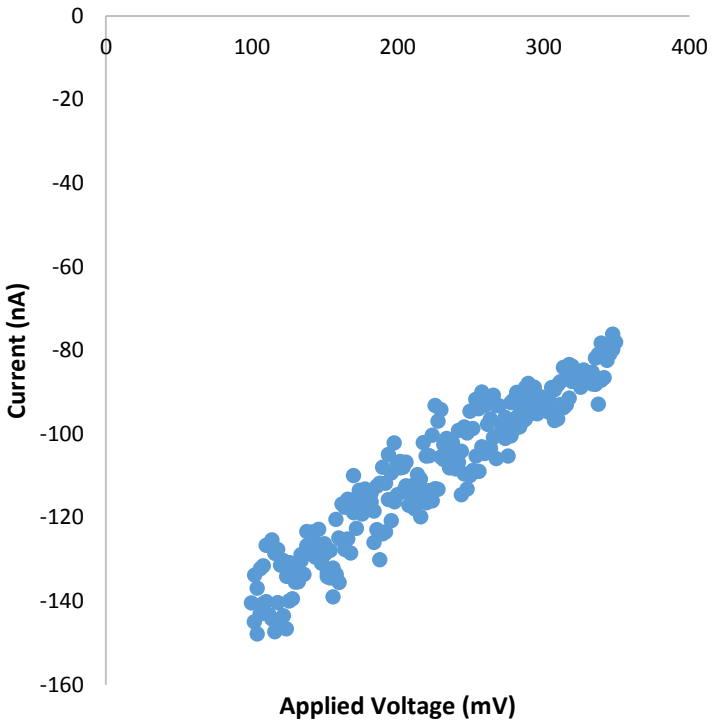

Fig. 48. CV After Testing for above titration curve

Appendix F: 3-mercapto-1-propane sulfonic acid

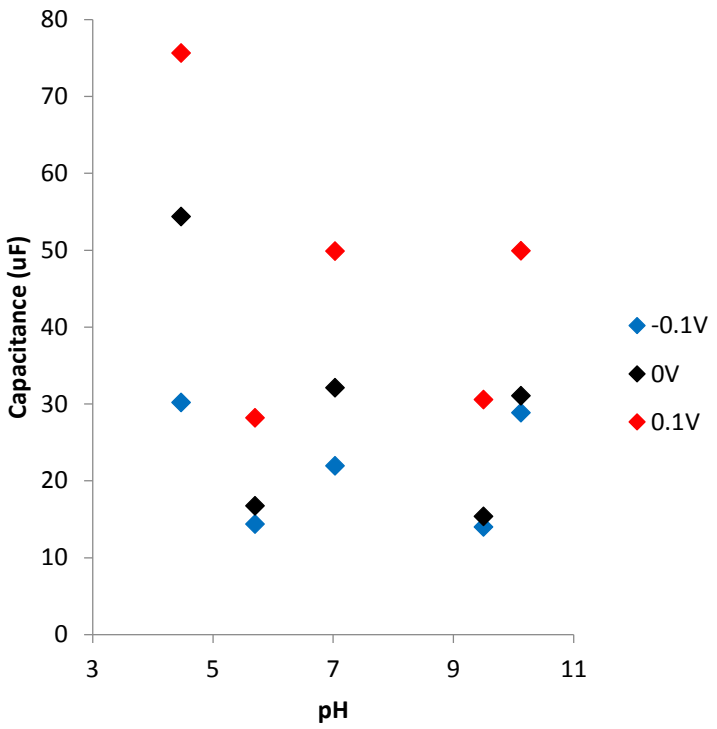

Fig. 49. 3-mercapto-1-propane sulfonic acid SAM made with literature procedure, bubbled with N2 and HCl, NaOH

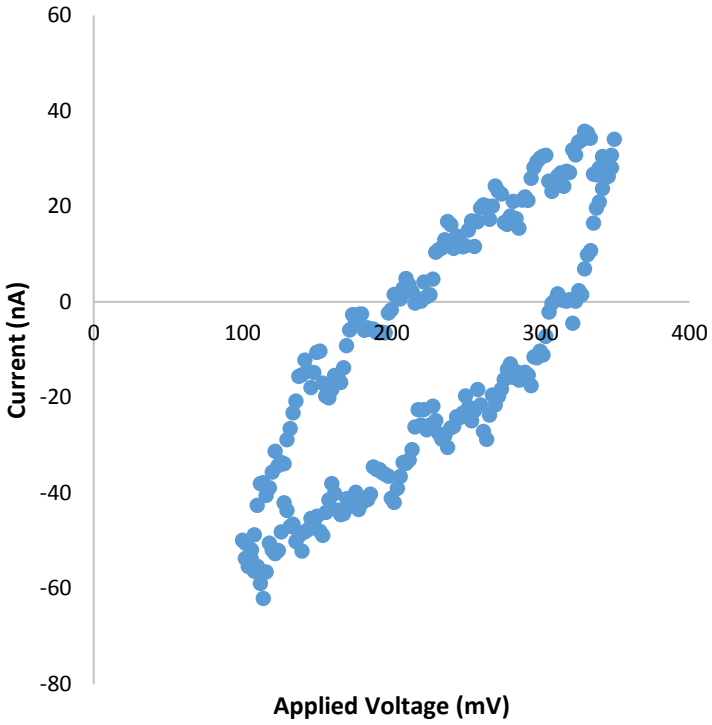

Fig. 50. CV Before Testing for above titration curve

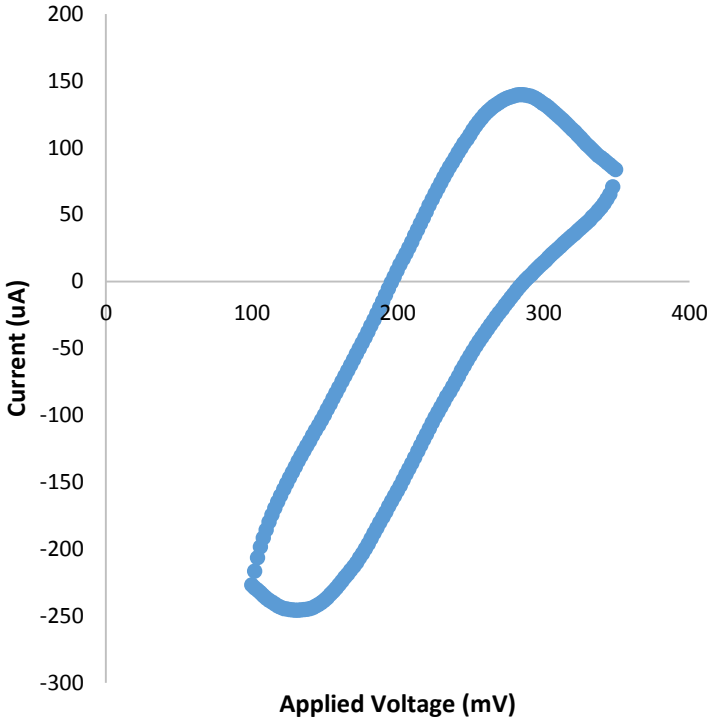

Fig. #51 CV After Testing for above titration curve

Table 3: CV data for SAM stability experiments

SAM Degredation % Chart						
Type	Min	Max	Range			
Au 1	-3.10E-04	1.88E-04	4.98E-04			
Au 2	-3.19E-04	1.95E-04	5.14E-04			
Au3	-3.23E-04	1.99E-04	5.22E-04			
Average Range			5.11E-04			
Gold Slide Above						
Sulfonic Acid Made According to Literature Before Testing DG 30min						
SA BF 1	1.90E-08	5.43E-08	3.53E-08			
SA BF 2	6.96E-08	8.99E-08	2.03E-08			
Average Range			2.78E-08			
Sulfonic Acid After Testing pH7, 0V, 5mV, 10k-3Hz 0 Day storage DG 30min						
SA BF 1	-2.95E-04	1.27E-04	4.22E-04			
SA BF 2	-2.95E-04	1.29E-04	4.24E-04			
SA BF 3	-2.93E-04	1.30E-04	4.23E-04			
Average Range			4.23E-04			
After % Degraded			82.7204			
Sulfonic Acid Made in Ethanol Backfilled DG 1hr 0 Day storage						
SA E 1	-6.85E-08	-2.79E-08	4.06E-08			
SA E 2	1.86E-08	4.72E-08	2.87E-08			
SA E 3	7.08E-08	9.87E-08	2.78E-08			
Average Range			3.23E-08			
SA in Ethanol Backfilled After pH7.2, 0V, 5mV, 10k-3Hz 0 Day storage DG 1hr						
SA E 1	-7.11E-08	-4.96E-08	2.15E-08			
SA E 2	-4.85E-09	2.13E-08	2.62E-08			
SA E 3	4.50E-08	6.70E-08	2.20E-08			
Average Range			2.32E-08			
After % Degraded			4.54E-03			
SA Made in Ethanol 1 Day Storage Slide 2 DG 1hr						
SA E 1	-3.12E-04	2.12E-04	5.24E-04			
SA E 2	-3.06E-04	2.26E-04	5.32E-04			
SA E 3	-3.01E-04	2.34E-04	5.35E-04			
Average Range			5.30E-04			
After % Degraded			1.04E+02			
Sulfonic Acid Made in Ethanol 1 Day Storage Slide 3 DG 1hr						
SA E 1	-7.81E-08	-5.05E-08	2.76E-08			
SA E 2	-2.49E-09	2.40E-08	2.65E-08			
SA E 3	5.25E-08	7.79E-08	2.53E-08			
Average Range			2.65E-08			
After % Degraded			5.18E-03			

Sulfonic Acid Made in Ethanol Slide 3 Exposed to Air 3 hrs DG 1hr						
SA E 1	-2.66E-04	1.36E-04	4.01E-04			
SA E 2	-3.27E-04	1.23E-04	4.49E-04			
SA E 3	-3.12E-04	1.36E-04	4.48E-04			
Average Range			4.33E-04			
After % Degraded			8.47E+01			
Sulfonic Acid Made in Ethanol DG 1hr						
SA E 1	-1.09E-08	8.43E-08	9.51E-08			
SA E 2	4.75E-08	1.38E-07	9.02E-08			
SA E 3	8.34E-08	1.66E-07	8.30E-08			
Average Range			8.94E-08			
Before % Degraded			1.75E-02			
Sulfonic Acid Made in Ethanol After 100k-0.1Hz EIS 0 Day storage DG 1hr						
SA E 1	-2.82E-04	1.89E-04	4.71E-04			
SA E 2	-2.84E-04	1.97E-04	4.81E-04			
SA E 3	-2.83E-04	1.96E-04	4.79E-04			
Average Range			4.77E-04			
After % Degraded			9.33E+01			
SA Ethanol Wash/SAM Solvent 0 Day Storage Slide 1 DG 1hr						
SA E 1	-1.03E-07	-3.89E-08	6.45E-08			
SA E 2	2.51E-08	9.67E-08	7.16E-08			
SA E 3	6.91E-08	1.31E-07	6.18E-08			
Average Range			6.60E-08			
Sulfonic Acid SAM Connected and Turned Off/On DG 1hr						
SA E 1	3.79E-08	1.08E-07	6.98E-08			
SA E 2	6.31E-08	1.33E-07	6.95E-08			
SA E 3	8.38E-08	1.49E-07	6.53E-08			
Average Range			6.82E-08			
After % Degraded			1.33E-02			
Sulfonic Acid SAM Connected and Software Switched						
SA E 1	8.32E-08	1.37E-07	5.37E-08			
SA E 2	1.65E-07	1.07E-07	-5.81E-08			
SA E 3	1.35E-07	1.99E-07	6.42E-08			
Average Range			1.99E-08			
After % Degraded			3.90E-03			
SA Ethanol Wash/SAM Solvent 2 Day Storage Slide 1 DG 30min						
SA E 1	1.64E-04	2.64E-04	1.00E-04			
SA E 2	1.69E-04	2.67E-04	9.80E-05			
SA E 3	1.52E-04	2.70E-04	1.18E-04			
Average Range			1.05E-04			
After % Degraded			2.06E+01			